

TOPICAL REVIEW • **OPEN ACCESS**

For the mitigation of urban heat island and urban noise island: two simultaneous sides of urban discomfort

To cite this article: I Kousis and A L Pisello 2020 *Environ. Res. Lett.* **15** 103004

View the [article online](#) for updates and enhancements.

You may also like

- [Interactions between urban heat islands and heat waves](#)
Lei Zhao, Michael Oppenheimer, Qing Zhu et al.
- [Shifting the urban heat island clock in a megacity: a case study of Hong Kong](#)
Xuan Chen and Su-Jong Jeong
- [A high density urban temperature network deployed in several cities of Eurasian Arctic](#)
Pavel Konstantinov, Mikhail Varentsov and Igor Esau

Environmental Research Letters



TOPICAL REVIEW

OPEN ACCESS

RECEIVED
13 May 2020

REVISED
22 July 2020

ACCEPTED FOR PUBLICATION
28 July 2020

PUBLISHED
28 September 2020

Original Content from
this work may be used
under the terms of the
[Creative Commons
Attribution 4.0 licence](#).

Any further distribution
of this work must
maintain attribution to
the author(s) and the title
of the work, journal
citation and DOI.



For the mitigation of urban heat island and urban noise island: two simultaneous sides of urban discomfort

I Kousis¹ and A L Pisello^{1,2}

¹ CIRIAF - Interuniversity Research Center, University of Perugia. Via G. Duranti 67—06125—Perugia Italy

² Department of Engineering—University of Perugia. Via G. Duranti 97—06125—Perugia Italy

E-mail: anna.pisello@unipg.it

Keywords: UHI mitigation, urban noise mitigation, urban discomfort, energy efficiency, cool materials, sound absorption, solar reflection

Abstract

Urban environment well-being has become a crucial public issue to face, given the huge concentration of population and climate change-related hazards at a city scale. In this view, Urban Heat Island (UHI) is now very well-acknowledged to be able to produce a serious threat to populations around the world and compromise human well-being due to aggressive overheating, exacerbated by anthropogenic actions. The same anthropogenic actions are also responsible for other discomfort causes such as noise pollution, which has also been demonstrated to heavily impact societal life and health conditions in urban systems. Both these phenomena typically co-exist in terms of space and time coincidence, and they both may be mitigated by means of smart adaptive and multifunctional surfaces including urban pavements and building envelopes. This review bridges the gap between only-thermophysical analysis about UHI mitigation and only-acoustics analysis of urban noise pollution, here defined as Urban Noise Island (UNI). To this aim, the key physics background of mitigation techniques is presented and the most innovative and promising solutions for counteracting UHI and UNI are described, with the final purpose to foster research and innovation towards more livable cities through a multiphysics and holistic view.

1. Introduction

In recent years, the steep rise of urbanization, a phenomenon referring to the population shift towards urban areas, has posed numerous challenges for the preservation of fair living standards for citizens around the world [1]. In 2016, 54% of the world population was reported as urban dwellers [2], while projections forewarn that in 2100 this fraction may be increased up to 85% [3]. At the same time, it is well documented that urban sprawl resulted in many cases of serious environmental issues within cities, which in turn put dwellers health in high-risk [4].

Among all environmental repercussions of urbanization, urban overheating is generally considered as the preeminent one [5–7]. Therefore, the typically high inner-city ambient temperature as compared to adjacent rural areas, i.e. Urban Heat Island (UHI), is a well-reported phenomenon occurring in many metropolitan areas. Being inherently interconnected with the ongoing Global Climate Change (GCC), UHI is a present-day issue accountable, in many cases, for inferior living standards occurrences within urban

areas [8–10]. Heat-related mortality and morbidity, expansion of air pollutants, high CO₂-eq emissions to the atmosphere, indoor/outdoor thermal discomfort, are some of the effects of UHI [9–11]. Yet, UHI effects are additionally magnified when interplay with heatwaves that increasingly occur within the last decades. [12–14]. In fact, more than 500 million urban dwellers are expected to undergo extreme heat-wave conditions once per five years [15]. Additionally, UHI implications may be perplexed even more with respect to diurnal and weekly temperature cycles which may vary according to the latitude and the time of day [16].

In view of that, release of anthropogenic heat [17–19], urban surfaces covered with dark-colored conventional materials [20, 21], complex concentrated urban structure, decreased sky view factor [22, 23] and alterations of urban evapotranspiration and convection efficiency [24] have been reported as the main drivers for UHI. In fact, metropolitan regions are mainly covered by pavements and buildings. For instance, McPherson [25] reported that pavements and buildings cover 50% and 25%

respectively of the commercial urban area of San Francisco, US while according to Akbari and Rose, paving surfaces may usually cover 35–40% of the total urban area [26]. As a consequence, the materials implemented in the urban infrastructure significantly regulate urban microclimate [27–29].

Yet, the vast majority of materials implemented in the civil environment, such as asphalt and concrete, are prone to high absorbance and thermal storage of the incident shortwave and longwave radiation. Hence they result in high superficial temperatures of pavements and building facades/roofs. [30, 31]. On that account, during the last decades, both academia and industry have investigated numerous types of materials capable of rejecting solar radiation as a countermeasure to UHI: traditional cool materials [32–34], natural cool materials [35, 36]; cool colored coatings [37–39]; cool membranes [40, 41]; cool materials enhanced with Phase Change Materials (PCMs) [42–44]; cool asphaltic materials [45–47]; fluorescent materials [48–50]; thermochromic pigments [51–53]; retroreflective skins [54–56]. Moreover, apart from employing the physical qualities of materials implemented in the urban environment, other strategies exploit greenery [57–59] and water bodies [60–62] potentiality of mitigating UHI, through evapotranspiration, sun direct shading and evaporation [63].

Still, urban overheating is not the only repercussion related to urbanization. The increased population density in urban areas inevitably led to another critical issue, such as high levels of anthropogenic noise [64]. The dense urban planning, mirroring the style of modern architectures, together with the exponentially increased need for urban transportation resulted in excessive noise incidences within cities [65]. As a result, cities are significantly louder than rural areas and thus can be regarded as Urban Noise Islands (UNI).

Urban noise is indeed observed in both developed and developing countries [66]. Already since 1994, a rough quarter of the total EU population had been reported as exposed to high transportation noise levels [67]. In 2011, one out of three European urban dwellers was reported distressed by urban noise incidences during its everyday routine [68]. This fraction rose up to 65% by 2013 [69]. More specifically, citizens were reported to systematically experience daily noise levels exceeding the upper limits (53 dB during day-time, 45 dB during night-time) established by the World Health Organisation [70]. Recent studies have moreover forewarned about the interconnection between high urban noise levels and severe impacts to humans' well-being such as stress [71] disturbed sleep [72], hearing loss [73] and increase of heart attack or stroke risk [74, 75].

In view of that, various measures have been promoted for counteracting UNI. The majority of them focus on the mitigation of transportation noise since

in most cases, it is liable for up to 80% of the total noise pollution in urban areas [76]. Low noise vehicle engines and tires, electric vehicles, effective traffic management, greenery solutions, reduction of traffic density, speed reduction, an overhaul of public transportation, and so forth [77–79] are among the main heretofore implemented solutions.

Nevertheless, unlike UHI, urban noise is not a well-documented phenomenon as it is. For instance, although several studies have highlighted UNI as a harmful problem and have proposed mitigation techniques on a small scale, according to the best of authors' knowledge, only a limited number studies has investigated holistic strategies for the mitigation of urban noise with respect to the mesoscale urban geometry and the built environment in particular [80, 81].

Since, however, the built environment dominates urban areas, there is a growing interest concerning materials incorporated in terms of further UNI mitigation potential. Under this scenario, novel or natural materials with noise mitigation qualities, e.g. sound absorption and control, have been investigated by a number of researchers [82–84]. Studies conducted in this scientific field have implemented noise absorbent materials that can be divided into two main categories; porous absorbers and resonance absorbers [85, 86]. The former is characterized by a wide absorption frequency range while the latter by a narrow range, particularly in the low frequencies. As a result, porous absorbers have been used into the urban environment especially in paving infrastructure for attenuating road-traffic noise which typically dominates within cities [83, 87]. In addition, porous media have been tested and found promising in terms of improving energy efficiency of buildings [88]. Moreover, within the last decades, advanced metamaterial structures have been developed with superior sound absorption, e.g. total sound absorption within a desired but rather narrow frequency range [89, 90]. However, their application is mainly at a theoretical level yet.

Within this framework, it becomes evident that urban materials and surfaces, in particular, may regulate urban microclimate and the corresponding multi-physical parameters. Thus, novel cross-cutting material-based measures could be taken for developing a more resilient and adaptive built infrastructure. Under this framework, novel smart materials, capable of multifunctionally improving urban environmental quality, could be considered as the next generation of urban smart skins.

In this regard, the main objective of this review study lays on a scientific challenge, which according to the best of the authors' knowledge, has not been faced yet: the multiphysics analysis of smart materials incorporated into the urban environment that can tackle both UHI and UNI at the same time and in the same spatial context, i.e. the anthropogenically

affected modern urban systems. Therefore, in this study, for the first time, a systematic review was carried out for presenting the scientific advances and techniques aiming to mitigate UHI and UNI which, out of the box, are characterized by different physical qualities. Nevertheless, their ongoing intensification has its origins on the materials incorporated into the urban environment. To that end, further on, this paper aims to discuss and suggest, under a conceptual framework, urban smart multifunctional surfaces that could conjoin simultaneously UHI and UNI offsetting qualities.

2. Methods and design

The review methodology of this study follows a systematic approach. The Systematic Review (SR) methodology is a research design for bringing together and critically analyzing results/findings from a list of strategically selected published studies. SRs originally emerged for collating outcomes of various experimental studies, especially ones related to health science field [91]. Yet, currently, their use is expanding towards evidence synthesis-based research methods aiming to give consolidate outputs, e.g. pinpoint scientific gaps/challenges and thus pave the way for future advancements of the relevant field. The main advantage of SRs compared to generic literature reviews lays on their quality of minimizing biases and random errors owing to a specific and predefined methodology typically consisting of the following 4 sub-steps:

- (a) Define a scientific question that needs to be answered.
- (b) Define explicit inclusion/exclusion criteria for the studies relevant to the topic to be reviewed.
- (c) Perform a critical review of the selected studies.
- (d) Conclude to research gaps/challenges and expound on future paths to be followed

Under this framework, at first, the following scientific question was defined as the main stimulus of this critical review study:

- Research Question: How can UHI and UNI be simultaneously mitigated by the same urban component?

Consequently, the following sub-questions were also defined in order to further structure the analysis.

- (a) What are the recent advances of applied material science in terms of UHI mitigation and relevant applications?
- (b) What are the main advantages/disadvantages of the above solutions in terms of UHI mitigation?
- (c) What are the recent advances of applied material science in terms of UNI mitigation and relevant applications?

- (d) What are the main advantages/disadvantages of the above solutions in terms of UNI mitigation?

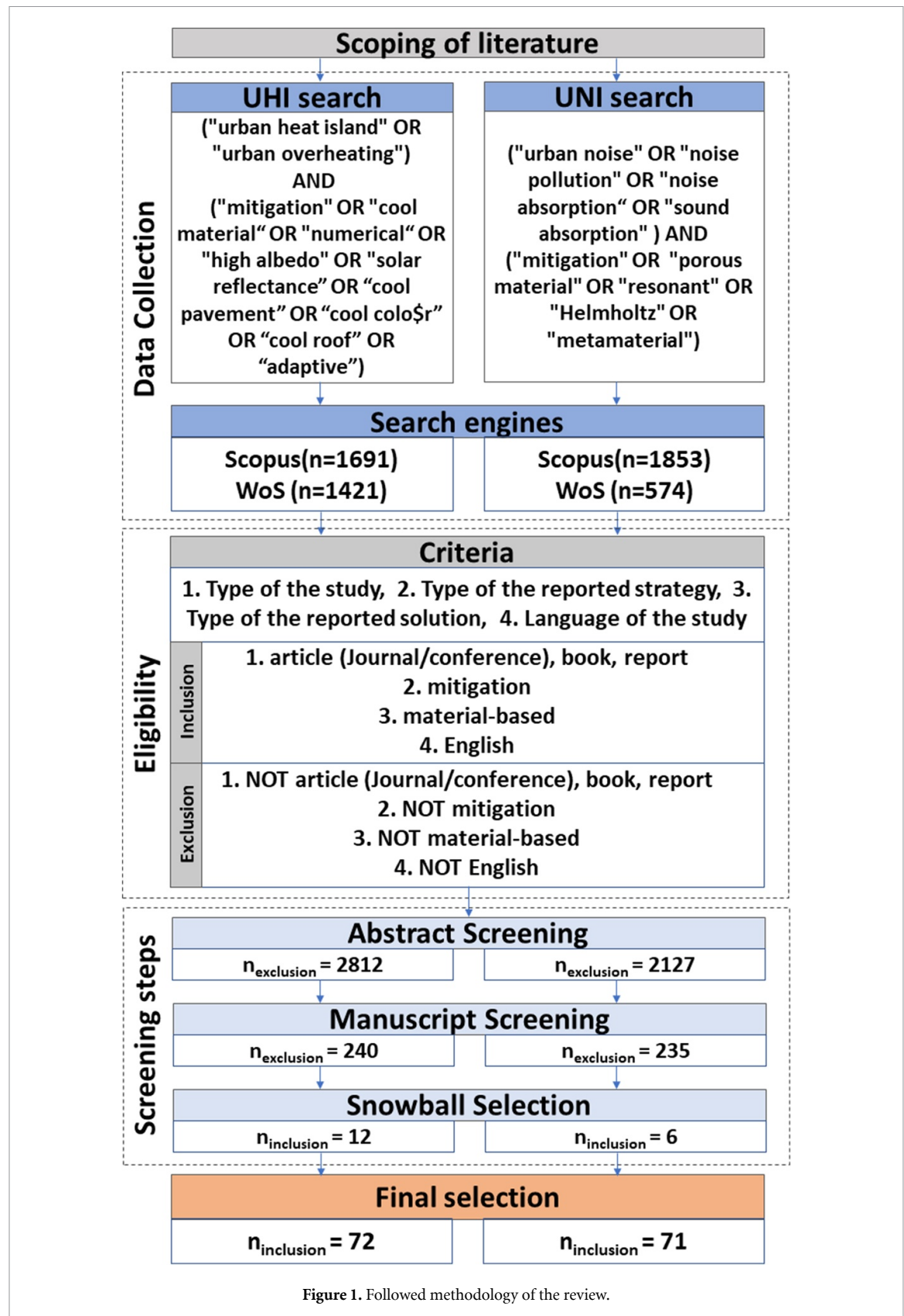
Scopus and Web of Science (WoS) were chosen as the primary web-search engines for the presented analysis. In addition, Google Scholar was utilized for identifying (i) grey literature (e.g. governmental documents and standards) related to the research questions, (ii) the work of key researchers according to the author's point of view and (iii) referenced publications found in previously reviewed publications within the presented review. The web search query was carried out within November 2019–February 2020.

Afterward, specific search terms related to UHI and UNI were determined and combined through the Boolean operators OR and AND for application to the scholarly databases (figure 1). The outcomes of both web academic databases were then merged and checked for duplicates. Subsequently, eligibility criteria were applied to the remaining publications for their exclusion/inclusion in the analysis (figure 1). In order to capture the historical continuity of the relevant advances, no time-frame exclusion criteria were applied. Yet, the vast majority (87%) of the reviewed studies come from 2006 to 2020 (figure 2). Furthermore, it should be noted that studies utilizing numerical models were considered for review only if the models were validated.

Finally, three screening steps were followed. Within the first step, studies for both UHI and UNI were included/excluded by reading the corresponding abstracts, while during the second step by reading the whole manuscript. Specific attention was given to journal articles since they were peer-reviewed. Within the last screening step, articles were retrieved through snowball selection [92]. In more detail, 12 and 6 publications concerning UHI and UNI respectively were not found directly within the results of the keywords search. Instead, they were identified through the reference lists of publications selected through the second screening test and their outcomes were considered of relevant significance. In the end, 62 journal articles, three conference articles, six technical reports and one book were reviewed in terms of UHI and 71 journal articles concerning UNI (table 1). One article was reviewed in terms of both UHI and UNI and therefore the overall number of the manuscripts included in the analysis was 142.

3. UHI mitigation

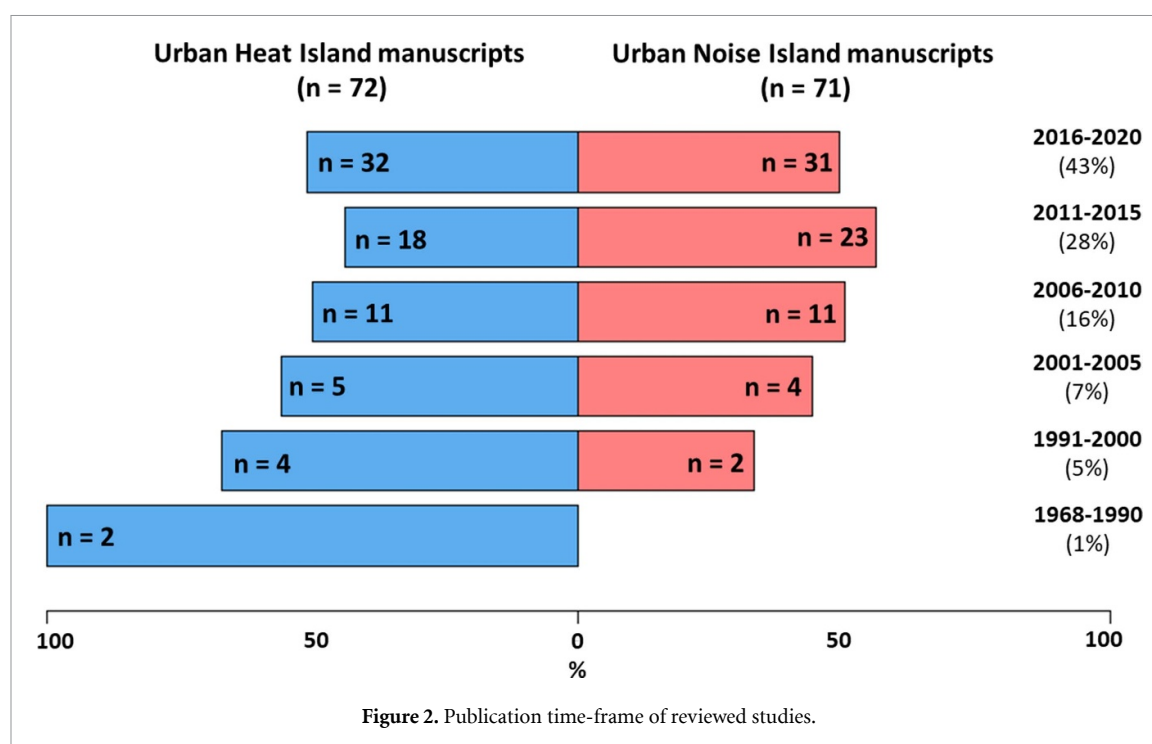
Hundreds of scientific studies have investigated techniques and synergies aiming at mitigating the hazardous effects of UHI on urban habitats [93, 94]. Furthermore, UHI is a well-investigated phenomenon not only at neighborhood or city scale but also on a global scale [95]. In fact, UHI may act synergistically with global climate change



and therefore its mitigation is considered of high importance not only by the scientific community but also by local and global authorities and policy-makers [96]. This chapter provides a snapshot of the scientific advances, utilized to date for cooling the cities [94].

3.1. Highly reflective materials

The first step towards the mitigation of UHI came off with the introduction of Cool Materials (CMs) (table 2). CMs' main attribute is high solar reflectance (also referred to as 'albedo' (α)) together with high emittance in the infrared spectrum [97]. This



reduces the solar energy gains of the surface, and increases the longwave radiative heat dissipation efficiency, and thus low surface temperatures can be achieved.

Towards the perspective of white CMs, in 1968, Givoni and Hoffman [98] compared grey colored building facades with white counterparts in terms of the superficial temperature. They showed that white-colored facades were approximately 3°C cooler under unventilated conditions. Later on, Berg and Quinn [99] measured the temperature of surfaces with different albedo values. They reported that an albedo value equal to 0.55 can result in a surface temperature almost equal to the ambient one. On the contrary, surfaces with a lower albedo (0.15) were almost 11°C warmer as compared to ambient temperature. The significance of the albedo value was reported also in the study of Taha *et al* [100]. They showed that an elastomeric coating characterized by albedo equal to 0.72 was up to 45°C cooler than a conventional black coating (albedo of 0.08).

Santamouris [104] reported that white-colored pavements, that naturally have higher albedo than dark-colored counterparts, can be up to 18°C cooler than conventional asphalt pavements. In the extensive study of Doulos *et al* [103] the thermal properties of 93 different paving materials were in-field investigated. Results showed that the materials' thermal balance is significantly related to their sunlight reflectivity and infrared emissivity. Moreover, it was concluded that the lighter the color of the surface, the higher the albedo and consequently the lower the surface temperature.

Within this framework, Synnefa *et al* [33] showed that a cool coating placed on a white concrete tile can decreased its surface temperature by 4°C and 2°C during daytime and nighttime respectively, under typical hot summers conditions. Similarly, Stathopoulou *et al* [32] reported that incorporating CMs into the paving and building infrastructure can significantly counteract UHI. CMs have been widely investigated as roof components. For instance, Akbari *et al* [101] reported that an increase of roof albedo by 40% may result in a reduction of roof temperature up to 22.2°C .

Moreover, Akridge [102] reported a roof temperature reduction by 33°C through the implementation of a high-albedo acrylic coating on a single floor building. Likewise, Pisello and Cotana [34] reported an up to 4.7°C indoor temperature reduction by implementing cool clay tiles on the roof of a non-insulated residential building in Italy. In addition, they showed that the winter penalty was negligible. Similarly, a minor winter penalty as compared to the annual energy savings concerning a cool roof application was reported also by Ramamurthy *et al* [105]. In more detail, they monitored the yearlong surface temperature and the corresponding heat flux of various roof structures with different albedo values on a test site located in Princeton, New Jersey, USA. Results also showed that during the summer period the surface temperature of white and black roofs ranged from 10°C to 48°C , and 10°C to 80°C respectively. The main determinant of heat loss during winter period was found to be the insulation thickness of the sub-layers.

Table 1. Type of reviewed manuscripts.

	Peer Reviewed Journal Articles	Peer reviewed Conference Articles	Technical reports	Books	Total
UHI	62	3	6	1	72
UNI	71	—	—	—	71

Table 2. Studies on high albedo materials.

Study	Year	Purpose	Outcomes
Givoni and Hoffman [98]	1968	white colored building facades compared with grey ones	3 K lower surface temperature
Berg and Quinn [99]	1978	superficial temperature of surfaces with various albedo	$a = 0.55$: temperature close to ambient $a = 0.15$: temperature 11 °C higher than ambient
Taha <i>et al</i> [100]	1992	superficial temperature of surfaces with various albedo	white ($a = 0.72$) was 45 °C cooler than black ($a = 0.08$)
Akbari <i>et al</i> [101]	1998	impact of roof albedo in buildings' cooling demand	22 °C lower temperature with 40% increase in roof's albedo
Akridge [102]	1998	high-albedo acrylic coating vs. conventional roof	33 °C decrease of roof peak temperature
Doulos <i>et al</i> [103]	2004	thermal properties of 93 commonly used pavement materials	“cold” materials = smooth and light colored and/or made of marble/mosaic/stone
Synnefa <i>et al</i> [33]	2004	reflective coatings vs. white tile	coatings were cooler up to 4 °C under hot summer conditions
Santamouris <i>et al</i> [97]	2008	low cost cool coating using lime vs. standard cool coating	15% increase in reflectance
Stathopoulou <i>et al</i> [32]	2008	properties of various building and paving materials	white coating ($a = 0.83$) up to 40 °C than black ($a = 0.04$)
Santamouris [104]	2013	white pavement vs. black asphalt	white was up to 18 °C cooler
Pisello and Cotana [34]	2014	cool roof for traditional building	indoor temperature decreased up to 4.7 °C

3.1.1. Microclimatic studies

In parallel, a large number of simulation studies have been carried out for evaluating the UHI mitigation potential of CMs (table 3). In one of the first approaches, Rosenfeld *et al* [106] implemented the Colorado State University Mesoscale Model (CSUMM) and showed that the replacement of dark-colored paving and building surfaces with high albedo counterparts could decrease peak summer temperature within Los Angeles area by 2–4 °C. Similarly, Rosenzweig *et al* [107] emphasized the significance of high albedo values concerning both roofs and pavements in New York City in terms of overall cooling potential. In fact, they utilized the Penn State/NCAR MM5 regional climate model and showed a potentiality of lowering the 2-meters air temperature by up to 2.9 °C. Similar findings were reported also by Lynn *et al* [108], who modified for this purpose the land surface model of National Centers for Environmental Prediction–Oregon State University–Air Force–Hydrologic Research Laboratory (NOAH LSM). However, this study also reported the risk of increasing pedestrian thermal stress during midday due to the high fraction of reflected solar radiation.

Taha [109] considered increases in roof, wall and pavements albedo over the area of Huston, US and

evaluated their impact by combining the standard and urbanized versions of the PSU/NCAR MM5 model. He showed that the cooling effect of a large-scale implementation of high albedo materials may exceed a 3 °C air temperature decrease. Furthermore, he reported the need for evaluating more aggressive albedo strategies. Towards this direction, Zhou and Shepherd [110] modelled the area of Atlanta, US with the Weather Research and Forecasting (WRF)-NOAH Land Surface Model (LSM) and concluded that tripling city's albedo could effectively attenuate UHI intensity. Similarly, Synnefa *et al* [111] performed numerical simulation for the city of Athens, Greece by utilizing the ‘urbanized’ version of the nonhydrostatic fifth-generation Pennsylvania State University–NCAR Mesoscale Model (MM5, version 3-6-1). They showed that by increasing the overall rooftops albedo to 0.63 (moderate scenario) and 0.85 (extreme scenario), an air temperature (2-m height) reduction of 1.5 °C and 2.2 °C respectively is feasible. Additionally, they highlighted that the overall mitigation potential could be substantially enhanced with the implementation of cool materials in the pavement and road infrastructure.

Ramamurthy *et al* [112] performed yearlong simulations with Princeton Roof Model concerning a

cool roof application in the New York City Metropolitan region. They showed that a highly reflective (albedo = 0.7) roof membrane can substantially decrease the annual energy demand. They also found out that the corresponding winter penalty is negligible since peak heating periods throughout winter period occur typically during night-time when albedo impact is trivial.

Zhang *et al* [95] utilized the version 1.2.0 Community System Model and perform an extensive study in terms of urban, continental and global scale. They reported, that except for some Africa and Mexico regions, a statistically significant annual and global mean temperature decrease varying from 1.6 to 1.2° C can be succeed. Another implementation of the Weather Research and Forecasting (WRF) mesoscale model concluded that an elevated albedo in Terni's urban structure may lead to a temperature decrease up to 2° C during both daytime and nighttime [113].

Further focus on the ageing issues of high albedo surfaces was given in the microclimatic study of Tsoka *et al* [114] through the implementation of ENVI-met for an urban district in the city of Thessaloniki. They reported that even though cool materials could reduce surface temperatures up to 9° C, a 10% reduction of their solar reflectance due to ageing could lead to a 50% reduction of their UHI mitigation potential. In another review study of the same scientific group [115] it was concluded that synergistic mitigation techniques in-between cool materials and trees can reduce the air temperature and the mean radiant temperature up to 2° C and 15° C respectively.

UHI is particularly responsible for an increasing trend of heat-related mortality within built-up areas, especially during heatwave periods [116, 117]. Within this framework, Macintyre and Heaviside [118] used the WRF regional weather model version 3.6.1 for evaluating the counteracting potential of an urban modification based on a cool roof intervention towards UHI within West Midlands, UK, and the consequent impacts to heat-related mortality. They found out that UHI is liable up to 40% of heat-related mortality during the summer period, while an extensive cool roof (albedo = 0.7) implementation could lead to a seasonal offset of 18%. This offset fraction was found even larger during heatwave periods, i.e. 25%. Additionally, they showed that for heatwave periods, cool roofs could decrease the downtown 2 m height air temperature up to 3° C, with an average decrease of 0.5° C.

3.1.2. Cool membranes

A number of studies aiming to counteract UHI effect focused on the development of cool roof membranes (table 4). For instance, Pisello *et al* [119], developed and analyzed both in-lab and in-field, cool membranes, characterised by solar reflectance equal to

85%. They emphasized that cloudy weather conditions, are a critical challenge for obtaining reliable results [119]. Additionally, Pisello *et al* [120] tested cool roof membranes and complementary cool facades on a university campus test building in Italy. This modification was found to decrease indoor temperature up to 3.1° C during cooling period.

Also, Phase Change Materials (PCM) have been embedded into cool roof membranes for optimizing indoor thermal comfort and reducing energy demand of the building [40]. In the study of Pisello *et al* [41], various alternative PCM concentrations were investigated for ameliorating ageing properties of cool roof membranes, while Saffari *et al* [43] conducted numerical simulations in order to determine the ideal PCMs melting temperature.

3.1.3. Natural cool materials

Several more eco-friendly or sustainable solutions have been reported as alternative passive cooling techniques, and, hence, capable of mitigating UHI (table 5). Pisello *et al* [35] quantified the cooling potential of several relatively inexpensive gravels implemented on both roof and pavement structures. By performing comparative experiments both in-lab and in-field, it was concluded that the highest reflectance of solar radiation (62%) was attributed to the grits with the finest grain size.

Castaldo *et al* [36] endorsed the aforementioned findings and concluded that the finest size stones preserve the higher indoor thermal comfort together with decreased energy demand. On a global scale, effective implementation of cool stone aggregates may also significantly counterbalance CO₂-eq emissions [36]. Moreover, natural stones have been reported to produce a significant evaporative cooling potential. For instance, Gonçalves *et al* [121] showed experimentally that natural stones can have in some cases a higher drying rate than the evaporation rate of a free water surface. In addition, evaporative cooling of natural stones implemented into built environment can protect built heritage from dampness and salt crystallization incidences.

3.2. Cool colored materials

In many cases, due to aesthetic or other reasons such as cultural heritage preservation, specific appearance should be preserved through colored materials and finishings. For that reason, scientists, apart from white high albedo materials, also developed cool colored alternatives (table 6). The principal idea behind cool colored materials lies in their ability to highly reflect the near infrared (NIR) part of the solar energy spectrum. In fact more than 50% of the incoming solar global radiation is included within the NIR wave-range [122]. As a result a cool material that (i) absorbs in the visible part for having its color, highly (ii) reflects in the NIR part and (iii) re-emits in the infrared part, can remain cooler than a

Table 3. Microclimatic studies on high albedo materials.

Study	Year	Purpose	Outcomes
Rosenfeld <i>et al</i> [106]	1995	albedo modification in Los Angeles	peak summertime temperature reductions between 2–4 °C with albedo increase of 0.13
Rosenzweig <i>et al</i> [107]	2006	impact of cool surfaces on New York microclimate	light colored surfaces can decrease air temperature up to 1.6 °C
Synnefa <i>et al</i> [111]	2008	impacts of large-scale increases in surface albedo on ambient temperature	1.5 °C and 2.2 °C temperature decrease with 0.63 and 0.85 albedo respectively
Taha [109]	2008	multi-day episode in August 2000 Texas, USA region	0.2, 0.05 and 0.12 increase of roof, wall and pavement albedo can decrease Tair up to 3 °C
Lynn <i>et al</i> [108]	2009	surface modification in New York	0.35 increase of pervious surfaces albedo can decrease Tair up to 2 °C
Zhou and Shepherd [110]	2009	first-order effects of UHI mitigation strategies	0.3 increase of pervious surfaces albedo can decrease Tair up to 2.5 °C
Zhang <i>et al</i> [95]	2016	potential global climate impacts of cool roofs	global adoption of cool roof ($a = 0.9$) may reduce UHI from 1.6 °C to 1.2 °C
Morini <i>et al</i> [113]	2016	surface modification in Terni, Italy	$a = 0.8$ for walls/roofs/roads may decrease UHI up to 2 °C
Tsoka <i>et al</i> [114]	2018	ground surface modification in Thessaloniki, Greece	$a = 0.4$ may decrease Tair up to 0.8 °C
Tsoka <i>et al</i> [115]	2018	evaluation of ENVI-met performance	synergistic UHI mitigation with cool-/greenery solutions may decrease Tair up to 2 °C
Macintyre and Heaviside [118]	2018	cool roof intervention in West Midlands, UK,	$a = 0.7$ may decrease Tair and heat-related mortality up to 3 °C and 25%

Table 4. Cool membranes.

Study	Year	Purpose	Outcomes
Pisello <i>et al</i> [119]	2016	in-lab/field analysis of waterproof cool roof membranes	85.4% solar reflectance
Pisello <i>et al</i> [40]	2016	polyurethane cool roof waterproof membrane with PCMs	Spectral reflectance/thermal emittance not compromised by PCMs
Pisello <i>et al</i> [41]	2017	optimize durability of polyurethane cool roof waterproof membrane with PCMs	durability optimization up to 25 wt%.
Pisello <i>et al</i> [120]	2017	cool coatings on differently oriented building envelope surfaces	$a = 0.51$ may improve indoor thermal comfort by 4.4 °C
Saffari <i>et al</i> [43]	2018	impacts of large-scale increases in surface albedo on ambient temperature	an optimized melting temperature of PCMs in cool membranes can reduce energy need without compromising durability

conventional colored counterpart that absorbs also in the NIR part and overall stores more energy. One of the first studies under this framework was performed by Levinson *et al* [123]. They developed several cool pigments of various colors able to absorb less than 10% of the NIR energy. Therefore, when these pigments are combined with the appropriate NIR background, they can function as a cool coating. In a study conducted by Synnefa *et al* [45], a practical substitution of conventional asphalt with cool colored asphalt base materials led to an average 5 °C decrease of ambient temperature. Likewise, Levinson *et al* [124] installed a near-infrared non-white reflective coating and reported a roof surface temperature decrease by 5–14 °C. As a result, Levinson *et al* [125] pointed

out the importance of increasing NIR reflectance for enhanced mitigation of UHI. Moreover, Doya *et al* [37] reported an 1.5 °C decrease of surface temperature on street facades by implementing cool selective paint.

Similar results were reported by researchers attempting to apply cool color strategies in historical/historic build environments. In order to maintain the building's external heritage, Rosso *et al* [127] implemented cool colored cement base materials which were found to decrease surface temperatures up to 8 °C and lower building energy demand as well. Equivalently, in a study of Rosso *et al* [38] concrete based materials characterized by significant NIR reflectance were implemented in historical buildings

Table 5. Natural cool materials.

Study	Year	Purpose	Outcomes
Pisello <i>et al</i> [35]	2014	characterization of low-cost grave coverings for roofs/paving	finest grain size has the highest solar reflectance (62%), highly reflective stone decreased its temperature by 5.5 °C compared to the commonly-used gravel
Castaldo <i>et al</i> [36]	2015	experimental and numerical analysis of low-cost grave coverings for roof-s/paving	depending on the grain size albedo can change up to 24%, global scale implementation: equivalent carbon emission offset of 4400 tCO ₂ -eq
Gonçalves <i>et al</i> [121]	2015	experimental evaluation of natural stone and ceramic brick as building components	limestones' drying rate was lower than the evaporation rate from a free water surface

Table 6. Cool-colored materials.

Study	Year	Purpose	Outcomes
Levinson <i>et al</i> [123]	2005	optical characterization of various pigments	colored materials that can reflect NIR (>90%) remain cooler in sunlight than comparable NIR-absorbing colors
Levinson <i>et al</i> [124]	2007	thermal performance roof tiles with NIR-reflective coatings	roof surface temperature decrease up to 14 °C
Levinson <i>et al</i> [125]	2007	methods for creating solar-reflective nonwhite surfaces	NIR reflectance's importance for UHI mitigation.
Syneffa <i>et al</i> [45]	2011	thermo-optical characterization of 5 color thin layer asphalt samples	surface temperature decrease up to 12 °C
Doya <i>et al</i> [37]	2012	application of cool selective paint on street facades	reduction of surface temperatures up to 1.5 °C
Song <i>et al</i> [126]	2014	effect of particle size distribution to NIR reflectance of TiO ₂ -based coatings	increasing the particles size leads to enhanced NIR reflection
Rosso <i>et al</i> [127]	2017	cool colored cement-based materials for maintaining buildings' external heritage	decrease surface temperatures up to 8 °C
Rosso <i>et al</i> [38]	2017	cool-colored concrete materials for historical areas' facades/pavements	up to 10.6 °C lower with respect to non-NIR samples
You <i>et al</i> [128]	2019	cool black membrane for asphalt	decrease surface temperature by 12.62 °C
Jin <i>et al</i> [129]	2019	Asphalt with PCM	reduction of the surface temperature up to 8.11 °C
Xie <i>et al</i> [130]	2019	thermo-optical properties of cool pavement nano-coatings	NIR reflectance = 95%, solar reflectance = 60%

and in building structure in particular. They were found capable of decreasing the surface temperatures up to 10.6 °C compared to the traditional clay bricks. You *et al* [128] developed a black coating with high near-infrared reflectance. In more detail, they effectively embedded CuO nanoparticles into black coatings and reported a surface temperature decrease of 12.62 °C as compared to a typical asphalt. Jin *et al* [129] exploit the latent heat properties of form-stable composite PCMs based on diatomite by embedding them into the asphalt. Results showed that during a typical summer day the superficial temperature of the asphalt may be reduced up to 8.11 °C, while the temperature rise can be significantly delayed.

Nano-scale based materials for building environment implementation are currently gaining popularity among academics due to their excellent optical properties. Recently, Xie *et al* [130] developed ten cool pavement coatings incorporating pigments including inorganic metal oxides of various particle sizes. The novel cool colored coatings were found able to highly reflect the NIR radiation, i.e. 95%, while preserving at the same time a fair solar reflection fraction, i.e. 60%. Optimization techniques related to the particle size of the pigments are ongoing as well. For instance, Song *et al* [126] researched the effect of various particle size distributions specifically to titanium dioxide rutile pigments for cool colored coatings. The distribution effect was found indeed significant; an

increased particle size leads to enhanced NIR reflection. Nonetheless, implementation of high-reflective pavement into urban environment is not trivial. In fact, their application may lead to thermal discomfort and/or glaring issues, e.g. when implemented in completely unshaded areas [131, 132]. Hence, their application should take place with respect to corresponding microclimate and boundary conditions and synergistically act with other passive cooling techniques and urban components such as trees and greenery.

3.3. Retroreflective materials

Another passive cooling technique for counteracting UHI, are the Retroreflective (RR) materials [133]. Unlike white and colored cool materials whose mechanism is based on diffuse reflection, RR are specifically designed to reflect the incident solar radiation directly back to its source [134]. Thus they preserve their cooling potentiality even if high rise structures are located in the packed surrounded area [135] (table 7).

In this context, Rossi *et al* [54] reported that RR can be even more effective in densely built areas as compared to traditional cool coatings. In order to further evaluate the impact of RR, Akbari and Touchaei, [136] developed a model that can estimate the hourly reflectance of directional reflective materials as a function of zenith and azimuth angles. RR materials' UHI mitigation potential was moreover noted by Han *et al* [55]. They examined the performance of a bio-inspired RR by means of dynamic simulation. The proposed RR as found capable of substantially decreasing the temperature of facing building surfaces and pedestrian air volumes.

Yuan *et al* [56] investigated RR in terms of ageing. They found that a prototype of RR including glass covering could maintain its initial reflectance and retro reflectance values (0.81 and 0.44 respectively) for over a year. Further in-lab and/or simulation comparative investigations concluded to RR superiority against conventional reflective materials concerning small scale application [56, 137].

An interesting comparison between RR and Diffuse Reflective (DR) material was carried out by Quin *et al* [138]. Walls enhanced with RR materials were found to maintain lower temperatures than walls with DR materials. However, their performance was substantially deteriorated when the incident angle of the sunlight on the surface exceeded 40°. A similar penalty with respect to the incident angle was reported also in the study of Yuan *et al* [139]. Further, Rossi *et al* [140] showed through an experimental campaign that RR surfaces can contribute towards the reduction of the energy kept inside urban canyons. In addition, they calculated and compared the energies remaining inside an urban canyon due to (i) RR and (ii) DR surfaces with similar global reflectance. A RR surface may indeed lead up to 37% decrease

of the remaining energy. However, as they pointed out, this result should not be considered as a representative one when it comes to real scale applications and moreover glare and light pollution issues should be further evaluated. A novel RR technique was introduced by Sakai and Iyota, [141]. They constructed RR materials able to reflect the incident light only during the summer period and thus capable of reducing cooling load and simultaneously rejecting the winter penalty. A similar approach was also proposed by Manni *et al* [142] who numerically investigated the potential application of selective RR materials into the urban canopy. The proposed RR materials were optimized according to the corresponding climate zone and latitude and were found to decrease the incident to urban surface radiation up to 50%.

3.4. Photoluminescent materials

Photoluminescent materials have been suggested as an alternative cooling method for mitigating UHI due to their intrinsic property to reject incident radiation not only by reflection but also by photoluminescence [48, 49] (table 8). Photoluminescence is a subcategory of luminescence and refers to the light emission from a matter, owing to the precedent absorption of photons. More analytically, when a molecule absorbs a photon in the visible region, it subsequently excites one of its electrons to a higher electronic excited state and then radiates a photon (i.e. releases energy), as the electron returns back to a lower energy state. Therefore, unlike conventional materials, photoluminescent materials, are characterised by a twofold rejection mechanism concerning incident radiation.

Photoluminescent materials were first proposed as a passive cooling technique in the study of Berdahl *et al* [49]. They investigated the fluorescent cooling of a ruby crystal (aluminum oxide doped with chromium) and proposed it as a robust fluorescent solution. Unlike the passive NIR-reflectance of the conventional cool colored materials, ruby was characterized by a deep red and near-infrared efficient emissivity as an active phenomenon. In fact, they overlaid white paint with a layer of ruby crystal which thus remained cooler than the reference, i.e. a conventional red coating, by up to 6.5° C. In the same study laser materials like ND-doped YAG, the cadmium pigments CdS, CdSe and their alloy fluorescence were also suggested as remarkable fluorescence examples.

Apart from the fluorescent materials which rapidly re-emit solar radiation, another subcategory of photoluminescent materials is the phosphorescent ones. These materials are characterized by a long-lasting emission of light, i.e. up to several hours later. While a small number of studies have investigated their lightning potential in road infrastructure [143, 144] their cooling potential has been investigated only in the study of Kousis *et al* [50]. In

Table 7. Retro-reflective materials.

Study	Year	Purpose	Outcomes
Akbari and Touchaei [136]	2014	development of a model for the hourly reflectance of directional reflective materials	Summer period: accurate estimation of mean hourly heat absorption and energy saving less than 40 W/m ² error for peak heat absorption, Winter period: less than 20% error for energy saving estimation 22 kJ/m ² and 9 W/m ² error for mean hourly and peak heat absorptions
Rossi <i>et al</i> [54]	2015	optic behaviour of RR materials in terms of angular reflectance for several inclination angles of solar radiation	higher cooling potential than traditional diffusive coatings
Han <i>et al</i> [55]	2015	effect of bio-inspired RR on building envelopes	average temperature reductions up to 0.46 °C
Yuan <i>et al</i> [135]	2015	durability of novel RRM for a period of 485 days	maintenance of initial reflectance (0.81), retroreflectance (0.44) for over a year.
Rossi <i>et al</i> [137]	2015	cool, white, diffusive material compared to white RR	during hot hours of the day the RR surfaces are 3–7 °C cooler
Qin <i>et al</i> [138]	2016	cool, white, diffusive material compared to white RR	when incident sunlight's angle exceeds 40 ° RR performance is deteriorated
Yuan <i>et al</i> [139]	2016	optical behavior of glass bead RR for application to building walls	sharply decreased performance at incident angles above 70 °
Rossi <i>et al</i> [140]	2016	white/beige traditional cool diffusive materials compared to RR	net (downward/upward) signal of RR and beige diffusive is 27 mV and 73 mV
Sakai and Iota [141]	2017	evaluation of novel high-reflective and ordinary RR materials	high-reflective RR: reflects light only during summer but is fragile Ordinary RR: weak retroreflectivity but it can withstand distortion
Manni <i>et al</i> [142]	2018	application of optimized selective RR materials	up to 50% decrease of the incident to urban surfaces radiation

more detail, they developed five concrete-based pavement fields with embedded phosphorescent components based on strontium aluminate with dysprosium and europium dopants and perform a monitoring campaign during the summer period for evaluating their cooling potential. They showed that the phosphorescent-based pavements can achieve up to 3.3 °C lower superficial temperature than a cool concrete field. Moreover, they concluded that further addition of phosphorescent components could lead to higher decrease in superficial temperature.

The results of Berdahl *et al* [49] and Kousis *et al* [50] suggest that the unique reflection-reemission mechanism, known as Effective Solar Reflectance, of photoluminescent materials is a promising technique for passive cooling applications and should be further exploited. Under this scenario, optimization of the experimental techniques for quantitatively measuring ESR is deemed necessary.

3.5. Thermochromic materials

Depending on the microclimatic characteristics of the implementation area cool materials could result to increased heating demand during the winter period [122, 145]. Under this framework, academics launched the "Thermochromic" Materials (table

9), i.e. materials capable to alter their color and thus their optical properties when their temperature reaches a predefined transition temperature value [146, 147]. As a result, a decreased heating/cooling demand during the cold/hot periods can be ensured [148].

Within this framework, Ma *et al* [149] placed thermochromic layers on a building facade and investigated their thermal behavior as well as their effect on indoor temperature. They reported that thermochromic coatings significantly reflected the incident solar radiation when the ambient temperature exceeded the transition temperature and as a result, interior thermal comfort was achieved. Karllessi *et al* [150] concluded to the same inference by benchmarking thermochromic coatings with both cool and conventional coatings during a cooling-demand period. Moreover, the thermochromic coating was found to maintain a lower mean surface temperature on a daily basis than the two counterparts. In this regard, Perez *et al* [51] developed a novel thermochromic mortar able to raise its reflectance in the visible spectrum as temperature rise, while simultaneously retaining constant values of reflectance in near-infrared area. Similarly, Hu and Yu [52] showed that a roof with thermochromic properties

Table 8. Photoluminescent materials.

Study	Year	Purpose	Outcomes
Berdahl <i>et al</i> [49]	2016	development and test of fluorescent cool-colored materials	6.5° C lower surface temperature than the conventional paint
Levinson <i>et al</i> [48]	2017	Test methods for measuring ESR	developed a computer-controlled rotary apparatus that measures ESR with a repeatability of about 0.02
Kousis <i>et al</i> [50]	2020	in-field monitoring of phosphorescent-based paving fields during summer period	up to 3.3° C lower surface temperature than cool concrete, phosphors delay peak surface temperature

can decrease heating/cooling demand and in parallel increase energy and cost savings up to 40.9% and 47.7% respectively. In another study implementing in thermochromic materials for roof applications, Fabiani *et al* [53], confirmed the winter penalty reduction potential both experimentally and numerically (by implementing the Princeton Urban Canopy model). Moreover, they showed that a superior stabilization of heat flux and temperature gradients can be ensured within each season, resulting in a higher quality thermal comfort for the building occupants.

Thermochromic solutions have been utilized in the pavement field as well. In the study of Yu and Hu [152] the thermal behavior of a thermochromic asphalt binder was examined. The novel binder was found able to maintain higher surface temperature during winter period in comparison with conventional asphalt and therefore was proposed as a snow deferring mechanism in cold climates. Generally speaking, however, thermochromic materials, are prone to photodegradation issues [150] that can significantly deteriorate their performance. For that reason, optimized thermochromic solutions have been developed with integrated red filter coverings [151]. Even though the coverings were found to delay the photodegradation further relevant research is needed for a large real-life implementation of thermochromics into the built environment.

3.5.1. Advanced nanoscale thermochromic and radiative cooling materials

Recently, nano-scale thermochromic solutions, based on Quantum Dots, Plasmonic, and Photonic structures were proposed as the next generation of cool urban materials in the study of Garshasbi and Santamouris [148] (table 10). Due to their non-bright nature, nano-scale materials can assert a pedestrian's visual comfort. In addition, since their properties are based on molecular rearrangement and nano-scale optical effects, they could counteract the photodegradation issues apparent on intermediate-scale materials [148]

Under this scenario, Garshabi *et al* [153], investigated the mitigation potential of a surface coated with Quantum Dots with high emittance in the infrared

wave-range. The results showed that the QDs coated sample was able to maintain a 10° C lower temperature than the reference sample. Quantum dots capped with TOP/TOPO/AET have been found to increase their photoluminescence intensity with temperature and vice versa, an effect known as thermal anti-quenching [154]. Therefore QDs are considered as a promising thermoresponsive cooling solution that needs to be further investigated [148].

At the same time, another promising technique for cooling applications, especially in hot and arid climates, is radiative cooling [155], i.e. structures that can highly reflect solar radiation while they behave almost as a black body within the atmospheric window wave-range (8–13 μm) [156, 157]. In recent years, plasmonic [158] and photonic [159] based prototypes have been tested for their radiative cooling potential. In their pioneering work, Raman *et al* [159], merged a photonic crystal structure and a thermal emitter and achieved sub-ambient temperature by 4.9° C during the hot hours of the day.

In another study concerning radiative cooling techniques, Zou *et al* [158], developed a plasmonic-based optical metasurface capable of decrease its temperature 7.4° C below the ambient temperature during day-time. It should be noted, however, that even though several studies have demonstrated exceptional cooling properties concerning radiative cooling mechanisms, little attention has been given to a possible implementation into the built environment. This can be of course explained by their relatively complex nature which makes their implementation non cost-effective.

3.6. Sustainable materials for mitigating UHI

In parallel, apart from developing novel materials for mitigating the UHI, research efforts have been attempted for maintaining a more eco-friendly approach (table 11). In fact, urban environment has been found responsible for almost 55% of the worldwide emitted greenhouse gases [160].

Under this scenario, Zinzi and Fasano [161] developed and tested a cool pigment made with a mixture of milk and vinegar. This novel pigment was found to decrease its surface temperature up to

Table 9. Thermochromic materials.

Study	Year	Purpose	Outcomes
Ma <i>et al</i> [149]	2002	investigation of chameleon-type building coatings	Winter: higher temperature by up to 3.5 °C than ordinary white building coating Summer: lower surface temperature by up to 4 °C than ordinary colored building coating
Karlessi <i>et al</i> [150]	2009	comparative analysis in-between thermochromic, highly reflective and common coating	Mean daily surface temperatures: 23.8–38.4 °C - thermochromic 28.1–44.6 °C - highly reflective 29.8–48.5 °C - common
Karlessi <i>et al</i> [151]	2013	optical filters for improving thermochromic durability	red filter, which cuts off wavelengths below 600 nm, protects most efficiently the reversible color change
Yu and Hu. [152]	2017	investigation of polymeric thermochromic materials into asphalt binder	Winter period: higher surface temperature than regular asphalt - ideal for delaying ice formation Summer period: cooling effect
Perez <i>et al</i> [51]	2018	smart mortar based on ordinary white Portland cement and organic microencapsulated thermochromic pigments	enhanced reflectance above transition temperature (31 °C) fine mechanical properties for building application
Xu and Yu [52]	2019	evaluation of thermochromic roof coating	decreased heating/cooling demand up to 40.9% and increased energy and cost savings up to 47.7%
Fabiani <i>et al</i> [53]	2019	evaluation of thermochromic roof with an Urban Canopy Model	annual stabilization of heat flux and temperature gradients, enhanced thermal comfort of occupants

Table 10. Advanced nano-scale materials.

Study	Year	Purpose	Outcomes
Raman <i>et al</i> [159]	2014	development of photonic solar reflector and a seven-layer thermal emitter	sub-ambient temperature by 4.9 °C during the hot hours of the day
Zou <i>et al</i> [158]	2017	radiative cooling design based on a dielectric resonator metasurface	7.4 °C below the ambient temperature during day-time
Garshasbi <i>et al</i> [153]	2019	QDs-based coating for UHI mitigation	10 °C lower temperature than the reference

20 °C compared to conventional enamel coating. In the study of Ferrari *et al* [162], a roof engobe was developed by commonplace materials, i.e. recycled glass and alumina for substituting conventional roof tiles in historical city-centers. The novel engobe was found to have an albedo value as high as 0.9. Also, waste bio-oils have been tested for paving application. Kousis *et al* [163], developed 4 novel paving binders made with waste palm oil and animal fat. They showed that the novel binders reflect more than 50% of incoming solar radiation within 750–1600 nm, i.e. significantly higher than typical asphalt and cement components. In addition, a binder made with animal fat was found to maintain up to 2 °C lower superficial temperature during the hottest hours of a summer day than the cool binder reference.

4. UNI mitigation

UNI mitigation strategies should focus on the main components of the Urban structure, such as the building envelope and pavements and the corresponding materials and finishing. The vast majority of the urban surfaces around the world consist of materials that can hardly absorb the incident soundwaves and thus intensify UNI by excessively propagating them. Recent advances in the field of acoustics, however, have set the foundations for urban components that can fairly mitigate noise and therefore moderate UNI. In this chapter, the recent advances, novelties, and strategies aiming to mitigate UNI and/or effectively control incident soundwaves are presented.

Table 11. Sustainable materials for mitigating UHI.

Study	Year	Purpose	Outcomes
Zinzi and Fasano [164]	2009	cool white paint obtained with a special mixture of milk and vinegar	up to 20 °C lower superficial temperature than the conventional
Ferrari <i>et al</i> [162]	2013	engobe manufactured by recycled glass and alumina	albedo equal to 0.9 was achieved
Kousis <i>et al</i> [163]	2020	development of cool paving binders with waste bio-oils	(i) solar reflectance > 50% within 750–1600 nm (ii) 2 °C lower surface temperature than cool reference during hot-hours of day

4.1. Porous materials

Porous absorbents are popular for reducing excessive indoor or outdoor noise incidences [165]. Their porous nature leads to thermal and viscous phenomena when the sound wave is propagated inside them. As a result, the noise wave energy is effectively dissipated. Nevertheless, their absorption abilities are undermined at low noise frequencies [83, 85, 166]. The energy conservation of the incident soundwave to the porous material can be described by [83]:

$$E_i = E_r + E_a + E_t \quad (1)$$

E_i where is the total incident sound energy, E_r is the sound energy of reflection, E_a is the sound energy of absorption, E_t is the sound energy of transmission.

Properties such as low-priced value and pliable nature made porous sound absorbers particularly popular among noise abatement tactics in urban environment [83, 87, 88]. Porous materials are generally divided in two main subcategories; (a) porous fibers and (b) porous foams. Their performance in terms of sound absorption is very much affected by materials' porosity (distribution and morphology of internal pores) and installation geometry, as well as the size and the position with respect to sources and receivers [167]. The main metric of sound absorption is the sound absorption coefficient which is defined as the fraction of absorbed to incident sound wave energy [168] and typically is represented by a :

$$a = \frac{E_a}{E_i} \quad (2)$$

4.1.1. Porous fibrous materials

Fibrous absorbing materials consist of chains of fibrous assemblies and depending on their nature can be classified as natural, inorganic, synthetic, metallic and nanofibers. Their main advantages compared with foam absorbers is their lightweight, elasticity and aesthetic appearance. Sound absorption properties of fibrous materials are determined by characteristic impedance Z_c [169]:

$$Z_c = \sqrt{\rho_e * K_e} \quad (3)$$

where, ρ_e is the effective density, K_e the bulk modules.

4.1.1.1. Natural porous fibers

In the study of Ersoy and Ku [170] industrial Tea-Leaf-Fibre (TLF) was investigated in terms of sound absorption. They showed that depending on the backing thickness of the TLF, its performance is comparable with, or even better than, polyester and polypropylene based non-woven fibre in terms of acoustic absorption potential. Similarly, Ismail *et al* [171] measured the sound absorption coefficient of four different thicknesses of *Aregna pinnata*. The results showed that 40 mm thickness is capable of 0.75–0.90 sound absorption coefficient within the range of 2000–5000 Hz.

In another study conducted by Fatima and Mohanty [172], jute and its composites were proposed, as another eco-friendly and cost-effective noise attenuation counterpart of glass fibre materials (table 12). Likewise in the study of Putra *et al* [173], natural waste fibers from paddy were proposed as a substitution of synthetic glass wool. Under the same scenario, sound-absorbing materials made of kenaf, wood, hemp, coconut, cork, cane, cardboard, and sheep wool were examined by Berardi and Iannace [174] with promising results at medium and high frequencies. Asdrubali *et al* [175] reviewed several natural unconventional sound absorbing materials for building implementation such as reed ($a > 0.5$ above 300 Hz), bagasse ($a > 0.5$ above 1000 Hz), wood panel manufactured with the addition of 10% rice straw wood ($a > 0.5$ above 1900 Hz) as well as recycled materials such as polyethylene terephthalate ($a > 0.6$ above 500 Hz) and bats made of recycled denim ($a > 0.95$ at 125 Hz). Waste bio-oils have also been tested for their sound absorption capability. In the study of Kousis *et al* [163] four novel paving binders were developed with palm oil and animal fat and used for developing corresponding paving specimens. Results from impedance tube showed that all novel specimens significantly outperformed typical asphalt and cements counterparts in terms of sound absorption.

Peng *et al* [176] studied the acoustic behavior of a material made of wood fiber and polyester fiber and concluded that by modifying the cavities length, the absorption peak can be modulated towards the desired frequency range. The importance of air cavity gaps for enhancing sound attenuation at lower frequencies was pointed out also in the study of Hee

Table 12. Natural porous fibers.

Study	Year	Purpose	Outcomes
Ersoy and Hurcuk [170]	2009	industrial Tea-Leaf-Fibre	$\alpha > 0.5$ above 1500 Hz
Ismail <i>et al</i> [171]	2010	Arenga pinnata fiber	$\alpha > 0.7$ within 2000 - 5000 Hz
Fatima and Mohanti [172]	2011	biodegradable and easily disposable natural fibre jute and its composite	$\alpha > 0.5$ above 1000 Hz
Putra <i>et al</i> [173]	2013	natural waste fibers from paddy	$\alpha > 0.5$ above 1000 Hz and $\alpha_{\text{average}} = 0.8$ above 1500 Hz
Berardi and Iannace [174]	2015	various natural fibers	kenaf fiber - $\alpha > 0.5$ above 800 Hz wood fiber - $\alpha > 0.6$ above 400 Hz hemp fiber - $\alpha > 0.5$ above 1100 Hz coconut fiber - $\alpha > 0.7$ after 400 Hz cork oak - $\alpha > 0.5$ above 1300 Hz Cardboard - $\alpha > 0.4$ above 400 Hz Sheep wool - $\alpha > 0.5$ above 400 Hz
Asdrubali <i>et al</i> [175]	2015	various natural and recycled fibers	reed - $\alpha > 0.5$ above 300 Hz bagasse - $\alpha > 0.5$ above 1000 Hz rice straw-based wood panel - $\alpha > 0.5$ above 1900 Hz polyethylene terephthalate - $\alpha > 0.6$ above 500 Hz recycled denim bats - $\alpha > 0.95$ at 125 Hz
Peng <i>et al</i> [176]	2015	composite material made of wood and polyester fiber	$\alpha > 0.5$ above 2000 Hz
Asdrubali <i>et al</i> [177]	2016	cardboard based panels	$\alpha < 0.5$ up to 5000 Hz
Hee <i>et al</i> [178]	2017	Fibres from the oil palm empty fruit bunch	$\alpha_{\text{average}} = 0.9$ above 1000 Hz.
Fabiani <i>et al</i> [179]	2018	performance of green roof substrates	the higher the RH the more the absorbance moves to higher Hz
Putra <i>et al</i> [180]	2018	extracted pineapple-leaf fibres	$\alpha_{\text{average}} = 0.9$ above 2000 Hz
Santoni <i>et al</i> [181]	2019	hemp fibrous materials	$\alpha > 0.5$ above 500 Hz and $\alpha > 0.8$ above 900
Kousis <i>et al</i> [163]	2020	paving specimens including binder made with animal fat or palm oil	$\alpha_{\text{average}} > 0.6$ within 500–1500 Hz (road-traffic noise)

et al [178] concerning a material based on oil palm empty fruit bunch fibres. Also, materials consisted of pineapple-leaf fibres and hemp fibres have been proposed as good sound absorbers [180, 181]. Similarly, Asdrubali *et al* investigated common reed-based panels for building envelopes and reported an overall poor absorbing performance, mainly due to limited porosity [177]. Another study carried out by Fabiani *et al* [179] focused on the acoustic performance of organic-based materials for green roof implementation within the Mediterranean region. Results showed that low relative humidity values help towards better sound absorption properties.

4.1.1.2. Inorganic porous fibers

4.1.1.3. Metal fibers

Inorganic fiber porous materials, such as fibrous metals, have attracted researchers' interest mainly due to their ability to maintain their properties under extreme conditions e.g. high temperatures and high levels of pressure [182, 183] (table 13). Therefore, various studies have investigated several metal-based sound-absorbing structures such as sintered fibrous metals [184], stainless steel fibrous felt materials [185, 186] and copper fibers [187]. Meng *et al* [184] examined rigid-backed sintered fibrous stainless steel

samples of different thicknesses in terms of sound absorption. They concluded that the smaller the diameter the higher the sound absorption coefficient which in fact can reach values almost equal to 1 for frequencies higher than 1000 Hz.

Similarly, Qingbo *et al* [185] showed that by decreasing the mean pore size of porous stainless steel fibrous felt materials their sound absorption properties can be significantly improved within the frequency range of 50-3500 Hz. In addition, an increase of 14.3% regarding sound absorption performance was reported for samples prepared at a sintering temperature below 850 °C. In another study concerning stainless steel metal fibrous materials, it was pointed out that a gradient pore structure is superior as compared to the regular pore ones in terms of sound absorption behavior [186].

Copper fibers have also been utilized in the study of Chen *et al* [187] for developing tri-dimensional reticulated porous material with fine sound absorption properties from 800 to 4400 Hz, i.e. sound absorption coefficient values reaching up to 0.94. It should be noted, however, that due to their fine mechanical properties under extreme conditions, fibrous metal materials are generally proposed for implementation in the field of aeronautics [183].

Table 13. Metal fibers.

Study	Year	Purpose	Outcomes
Bo and Tianning [182]	2009	porous sintered fiber metal	$\alpha > 0.9$ within 1700-6400 Hz
Sun <i>et al</i> [183]	2010	effect of high temperatures on absorbing properties of fibrous metal materials	$\alpha > 0.8$ within 1500-6500 Hz
Meng <i>et al</i> [184]	2015	sintered fibrous metals	$\alpha > 0.7$ within 1500-6500 Hz
Qingbo <i>et al</i> [185]	2015	Porous stainless steel fibrous felt materials	$\alpha > 0.6$ within 2000-3000 when sintered at 850 °C
Zhu <i>et al</i> [186]	2016	optimization of metal fiber porous materials	a gradient pore structure significantly improves sound absorption compared to regular porous samples
Chen <i>et al</i> [187]	2017	tri-dimensional reticulated porous material made of copper fibers	$\alpha > 0.5$ above 1100 Hz

4.1.1.4. Synthetic porous fibers

4.1.1.5. Nonwoven fibers

A polyethylene terephthalate (PET), thermoplastic polyurethane (TPU) honeycomb grid, and polyurethane (PU) foam-based sandwich plank was manufactured by Lin *et al* [188] and found to have an average sound absorption coefficient of 0.77 within 0-4000 Hz. Other studies scrutinized the acoustic performance of polyester and polypropylene nonwoven selvages [189], recyclable flame retardant nonwoven [190] islands-in-the sea fibers [191], high-loft nonwoven fibers [192]. The dependence of sound absorption coefficient on different fiber blend ratios and bulk densities has been examined as well [193]. However, the result showed that in general, materials exhibit little sound absorption properties in the low and medium frequency range which is the most critical for humans health (table 14).

4.1.1.6. Nanofibrous additions

Nanofibrous additions have been found to optimize the sound absorption mechanism of traditional acoustic materials in the low and medium frequency range (table 15). This was reported in the study of Xiang [194] wherein perforated, panel, foam and fiber-based materials were enhanced with electrospun polyacrylonitrile nanofibrous membranes. Similarly, Kucukali-Ozturk *et al* [195] reported sound absorption coefficient values up to 0.7 in the low and mid-frequency values by placing electrospun polyacrylonitrile-based nanofibers on specimens. Substantial sound attenuation properties within 400-900 Hz were reported also in the study of Chang *et al* [196] who launched a novel methodology for creating 3D nanofibrous networks. Similarly, in other relevant studies, it was demonstrated that electrospun piezoelectric Polyvinylidene fluoride (PVDF) membranes may not only substantially absorb noise at low frequencies, but also convert sound energy to electric potential [197, 198].

4.1.2. Porous foams

Porous foams absorbers are consisting of interconnected cellular structures and depending on their

chemical composition can be classified as organic, inorganic and hybrid. They are widely used in the urban environment due to their low manufacture cost.

4.1.2.1. Porous Hybrid Foams

Wu *et al* [199] reported a significant sound attenuation at low frequencies by implementing graphene foam (GF)/carbon nanotube (CNT)/poly (dimethyl siloxane) (PDMS) composites. In fact, they achieved over 30% sound absorption in the frequency range of 100-1000 Hz and 70% in the range of 100-200 Hz. Porous metal foams have also been examined for their sound absorption capabilities. Bai *et al* [200] examined 5 different porous metal absorbers; original porous metal, compressed porous metal, compressed and microperforated porous metal panel, microperforated spring steel panel, and microperforated uncompressed porous metal. It was noted that the compressed and microperforated porous metal panel absorber with a cavity length of 20 mm is capable for an average 59.69% sound absorption in the range of 100-6000 Hz, i.e. 25.70% higher than the original porous metal absorber (table 16).

4.1.2.2. Porous Organic Foams

Flexible polyurethane foams (FPF) have been widely regarded as a fine example of organic foam with significant sound absorption properties [201, 202] (table 17). Moreover, it has been reported that the sound absorption properties of flexible polyurethane foams can be further enhanced with the addition of fluorine-dichloroethane and triethanolamine [203]. Other flexible polyurethane foams alterations have also been proposed as good sound absorbers, due to the inclusion of uretonimine contents [204], high molecular weight copolymer polyol [205], wood fibers [206] and high molecular weight isocyanate contents [207].

On the other hand, one of the first efforts aiming to construct environmentally friendly porous foams was carried out by Mosanenzadeh *et al* [208]. They reported that better sound absorption

Table 14. Nonwoven fibers.

Study	Year	Purpose	Outcomes
Lou <i>et al</i> [189]	2005	polyester and polypropylene non-woven selvages	$\alpha > 0.5$ above 1184 Hz
Kosuge <i>et al</i> [190]	2005	A flame retardant nonwoven fabric made with para-aramid fibre and polyester fibre sintered fibrous metals	when attaching para-aramid paper with less than 30 cc/sec/cm ² of permeability to nonwoven fabric, α above 2000 Hz was better than that of glass wool and above 0.6
Suvari <i>et al</i> [191]	2013	spunbonded nonwovens made with Nylon 6 (PA6) and polyethylene	$\alpha > 0.1$ above 4500 Hz
Zhu <i>et al</i> [193]	2015	Thermally Bonded Nonwovens	$\alpha > 0.5$ above 1250 Hz
Suvari <i>et al</i> [192]	2016	Thermally bonded high-loft nonwovens with minimum thickness	$\alpha > 0.5$ within 2000 -6000 Hz for 1575 g/m ² samples thickness range 10-50 mm

Table 15. Nanofibrous additions.

Study	Year	Purpose	Outcomes
Xiang <i>et al</i> [194]	2011	electrospun polyacrylonitrile (PAN) nanofibrous membranes placed on BASF foam and glass fibers	BASF foam/Glass fiber improved both $\alpha > 0.5$ above 1900 Hz
Kucukali-Ozturk <i>et al</i> [195]	2015	Polyacrylonitrile nanofibers electrospun on spacer-knitted fabrics by varying deposition amount and surface coating arrangement	$\alpha = 0.7$ at the low and medium frequency range
Chang <i>et al</i> [196]	2016	3D nanofibrous networks, featured with neutralization and self-assembly of electrospun nanofibers	$\alpha > 0.5$ above 410 Hz
Wu and Chou [197]	2016	porous piezoelectric PVDF materials	$\alpha > 0.5$ above 900 Hz
Wu and Chou [198]	2016	electrospun polyvinylidene fluoride/-graphene membranes	$\alpha > 0.5$ above 700 Hz

Table 16. Porous Hybrid Foams.

Study	Year	Purpose	Outcomes
Wu <i>et al</i> [199]	2017	graphene foam/carbon nanotube/poly(dimethyl siloxane) composites	$\alpha = 0.7$ at 100–150 Hz
Bai <i>et al</i> [200]	2019	absorbers fabricated by the compression and microperforation of porous metal	$\alpha_{\text{average}} = 0.6$ within 100–6000 Hz

performance can be achieved, by substituting the non-recycling polyurethane with polypropylene as a recyclable thermoplastic polymer, and polylactide as a bio-based thermoplastic polymer made from renewable resources. Another novel graded bio-based foam structure capable of enhancing the noise attenuation in wider frequency range as compared to uniform foams has been introduced also by Mosanenzadeh. [209].

4.1.2.3. Porous inorganic foams

Inorganic foams (table 18) are typically used for sound absorption applications in harsh environments (e.g. aerospace and marine industry) [210]. Towards this direction, acoustic absorption properties of foams based on open-cell Al alloy [210], alumina and alumina/trifunctional epoxy composites [211], open-cell metallic [82], porous zeolite [212] and

Si₃N₄ ceramics [213] have been examined. Results showed promising results concerning sound absorption, especially in high frequencies. For example, Ke *et al* [210] increased the sound absorption of open-cell Al alloy foams with graded pore size by introducing an air gap behind the foam. The resulted absorption coefficient was higher than 0.5 within 300 to 1100 Hz. Cuiyun *et al* [212] fabricated porous zeolite specimens through sintering process by mixing zeolite powder with polymer foam particles which were found capable of absorbing more than the 50% of the incident soundwave above 850 Hz. Similar results were reported by Ligoda *et al* [211] concerning alumina foams within the frequency range above 1200 Hz, while Zhai *et al* reported a sound absorption coefficient higher than 0.9 within 1500–6000 Hz for an open-cell IN625 metallic foam of 50 mm thickness.

Table 17. Porous Organic Foams.

Study	Year	Purpose	Outcomes
Lee <i>et al</i> [202]	1991	Flexible Polymeric Foams	$\alpha > 0.9$ at 1000 Hz
Sung <i>et al</i> [201]	2007	optimized flexible polyurethane foam with various plate-like fillers	$\alpha > 0.6$ above 2000 Hz
Mosanenzadeh <i>et al</i> [208]	2013	polymeric open cell foams from polypropylene(PP) and polylactide (PLA) resin	$\alpha > 0.5$ above 3000 Hz for PP $\alpha > 0.6$ above 2000 Hz for PP
Mosanenzadeh <i>et al</i> [209]	2015	graded bio-based foam structure	$\alpha > 0.6$ above 2000 Hz
Chen <i>et al</i> [203]	2015	Additive components for the optimization of Polyurethane Foams	$\alpha > 0.6$ above 700 Hz with foaming agent 141b
Sung <i>et al</i> [204]	2016	Effect of isocyanate molecular structures in fabricating flexible polyurethane foams	the higher level of uretonimine content the lower the value of α
Sung and Kim [207]	2017	Effect of high molecular weight isocyanate contents on manufacturing polyurethane foams	$\alpha > 0.5$ above 1000 Hz and $\alpha > 0.9$ around 2000 Hz
Sung <i>et al</i> [205]	2018	flexible polyurethane foams including high molecular-weight copolymer polyol	$\alpha > 0.5$ above 750 Hz
Choe <i>et al</i> [206]	2018	wood fibers to enhance the sound absorption coefficient of flexible polyurethane composite foams	$\alpha > 0.5$ above 1000 Hz and $\alpha > 0.9$ around 2000 Hz

Table 18. Porous Inorganic Foams.

Study	Year	Purpose	Outcomes
Ke <i>et al</i> [210]	2011	open-cell Al alloy foams with graded pore size	$\alpha > 0.5$ within 300–1100 Hz
Cuiyun <i>et al</i> [212]	2012	zeolite powder and polymer foam particles	$\alpha > 0.5$ above 850 Hz
Wang <i>et al</i> [213]	2017	Highly porous Si3N4 ceramics	$\alpha > 0.5$ above 1200 Hz
Ligoda <i>et al</i> [211]	2017	alumina foam/tri-functional epoxy resin composites vs. alumina foam	Alumina foam: $\alpha > 0.5$ above 1200 Hz Alumina/epoxy composite: $\alpha > 0.5$ within 2000–3100 Hz
Zhai <i>et al</i> [82]	2018	open-cell metallic foams	$\alpha > 0.9$ within 1000–6000 Hz

4.2. Resonant sound absorbers

Resonant absorbers can ensure fair sound absorption properties at low to mid frequencies, where porous absorbers usually fail to achieve significant absorption due to the internal resonance effect [85]. More specifically, their resonant frequency can be tuned to a specified value in which sound absorption will be maximized [166]. This property however, makes them efficient in terms of sound absorption only for a narrow frequency band [85, 214, 215].

There are two common forms of resonant absorbers: membrane/panel absorber and Helmholtz absorber. For a membrane/panel absorber, the mass is a vibrating sheet of membrane or panel made from various materials. The spring is usually provided by the resilient boundary of the membrane or panel or air enclosed in the cavity. In the case of a Helmholtz absorber, the mass is a plug of air in the opening of a perforated sheet and the spring is usually provided by air enclosed in the cavity.

4.2.1. Membrane/panel absorber

A micro-perforated panel (MPP) (table 19) consists of a thin sheet panel perforated with a lattice of

sub-millimetre apertures which creates high acoustic resistance and low acoustic mass reactance. Both are necessary for broadband sound absorption without further using additional porous material [216]. In the past decades, high manufacturing cost [215] of MPP was a critical disadvantage for their wide implementation. Nevertheless, recently, several recyclable materials have been proposed for MPPs manufacture leading to their sound absorption properties exploitation [217]. Therefore, many scientists tend to regard them as superior solutions than traditional porous materials [218]. The acoustic impedance of a micro-perforated panel, with either circular or slit cross-section, can be approximated as [216, 219]:

$$Z_{\text{circular}} \approx \frac{32\eta t}{d^2} \sqrt{1 + \frac{k_c^2}{32}} + i\rho_0\omega t \left(1 + \left(3^2 + \frac{k_c^2}{2} \right)^{-\frac{1}{2}} \right) \quad (4)$$

$$Z_{\text{slit}} \approx \frac{12\eta t}{d^2} \sqrt{1 + \frac{k_s^2}{18}} + i\rho_0\omega t \left(1 + (5^2 + 2k_s^2)^{-\frac{1}{2}} \right) \quad (5)$$

where t is panel thickness, d is perforation diameter, η is the dynamic viscosity coefficient, ω is the angular frequency, ρ_0 is the density of air, and k_c and k_s are the perforation constants for the circular and slit cross-section respectively.

Cobo and Espinosa [215] introduced a novel fabrication technique of MPPs with good performance in mid to high-frequency range, i.e. absorption coefficient values above 0.8 within the frequency range of 1600–2600 Hz. Aiming to magnify the noise attenuation in lower frequencies, Li *et al* [220, 221] proposed the use of perforated panel with extended tubes in unison with a porous material. The designed structure was found capable of significantly absorbing soundwaves from 300 to 1100 Hz (sound absorption coefficient values varied from 0.6 to almost 1). Similarly, Bucciarelli *et al* [222] developed a multilayer microperforated panel able to highly absorb sound in lower frequencies. Their study demonstrated a sound-absorbing structure comprised of six plastic micro-perforated panels with constant absorption properties over 90% from 400–2000 Hz. Another novel structure with perforated honeycomb-corrugation hybrid sandwich panels with fair noise reduction performance in low frequencies has been proposed by Tang *et al* [223]. By implementing the Simulated Annealing algorithm, they demonstrated an average sound absorption coefficient equal to 0.75 in the range of 500–1000 Hz together with fine mechanical properties.

4.2.2. Helmholtz resonator

The Helmholtz Resonator (HR) (table 20), which consists of a cavity communicating with an external duct through an orifice, is a well-known device to reduce noise centralized in a narrow band at its resonance frequency [224]. For a single neck Helmholtz resonator, the resonant frequency, f_r is given by:

$$f_r = \frac{\nu}{2\pi} \sqrt{\frac{A}{L'V}} \quad (6)$$

where L' and A are the length and the area of its neck respectively, V is its volume, and ν is the soundspeed. The acoustic impedance is given by:

$$Z_a = R_a + jX_a \quad (7)$$

where R_a is the acoustic resistance of the absorber, which is related to the porous material used in the cavity and/or the viscous loss along the neck. X_a is the acoustic reactance of the absorber and can be calculated with respect to the mechanical reactance of the system by:

$$X_a = (\omega M_a - \frac{K_a}{\omega}) \quad (8)$$

where M_a is the mass of the air inside the neck, ω is the angular frequency, and K_a is the acoustic stiffness of the cavity.

Under this scenario, Chen *et al* [225] demonstrated a great improvement in terms of transmission loss by adding HRs into a duct. This was succeeded in specific frequencies, i.e. 28 dB and 18 dB for 250 Hz and 500 Hz respectively, by placing specially designed band-pass filters. In a study of Tank [226] HRs sound absorption properties were enhanced by introducing a neck tapering technique. He found out that the deeper the tapering the higher the sound absorption coefficient which can reach values above 0.8 in the frequency range of 80–100 Hz. Similarly, Esteve and Johnson [227] demonstrated an overall decrease of 7.7 dB in the 50–160 Hz range by coupling distributed vibration absorbers and HRs into a cylindrical enclosure.

HRs have also been proposed for window implementation [228]. The proposed double glazed window structure was found capable of decreasing the transmitted sound pressure levels within 50–120 Hz. In general, HRs have been further utilized for tackling the low-frequency penalty of sound absorption MPPs. For instance, Park [229] backed MPP with HRs and succeeded an overall reduction of 7.9 dB within 25–630 Hz. Similar approaches have been reported from several scientific groups with successful results opening the way for further application of resonant sound absorbents [84, 230] in terms of noise mitigation.

4.3. Metamaterials

The latest frontier in the evolution of acoustic absorption materials is the development of acoustic metamaterials. Unlike natural porous and resonant absorbers, acoustic metamaterials are artificial materials with advanced acoustic properties compared to their natural counterparts. For example, while effective mass density and bulk modulus of conventional materials are always positive, when it comes to metamaterials their values can be also negative [231–233].

In general, the effective mass is described by [234]:

$$D_{\text{eff}}V = M_0 + \frac{m\omega_0^2}{\omega_0^2 - \omega^2} \quad (9)$$

where D_{eff} is the effective density, V is the total volume, ω_0 is the resonant frequency, ω is the angular frequency of the time harmonic excitation, and M_0 and m are the mass of the matrix and the solid components, respectively.

Moreover, in the framework of Effective Medium Theory (EMT), the effective bulk modulus of fluid and solid composite structures B_{eff} is [235]:

$$\frac{1}{B_{\text{eff}}} = \frac{1-f}{B_1} + \frac{f}{B_2} \quad (10)$$

Table 19. Membrane/panel sound absorbers.

Study	Year	Purpose	Outcomes
Cobo and Espinosa [215]	2013	cheap microperforated panel absorbers	$\alpha > 0.5$ within 1200–3400 Hz $\alpha > 0.9$ within 1600–2250 Hz
Li <i>et al</i> [221]	2016	perforated panel with extended tubes (PPET)	three parallel-arranged PPETs combined with a MPP have $\alpha > 0.6$ within 200–440 Hz
Li <i>et al</i> [220]	2017	compound sound absorber comprised of perforated plates with extended tubes (PPET) and a PSAM for improving α within 100–1600 Hz	$\alpha > 0.8$ within 200–350 Hz $\alpha > 0.6$ within 600–900 Hz
Tang <i>et al</i> [223]	2017	ultra-lightweight sandwich panel with perforated honeycomb-corrugation hybrid (PHCH) core	average $\alpha = 0.75$ within 500–1000 Hz
Bucciarelli <i>et al</i> [222]	2019	multiple layer MPP absorber	sound absorption over 90 % within 400–2000 Hz

Table 20. Helmholtz resonator.

Study	Year	Purpose	Outcomes
Chen <i>et al</i> [225]	1998	improvement on the acoustic transmission loss of a duct by adding Helmholtz resonators	improvement of almost 28 dB at 250 Hz
Esteve and Johnson [227]	2002	model study on a set of distributed vibration absorbers and Helmholtz resonators applied to a cylindrical enclosure	decrease of 7.7 dB in the 50–160 Hz
Tang [226]	2005	Helmholtz resonators with tapered necks	$\alpha > 0.8$ within 80–100 Hz
Mao and Pieztrko [228]	2010	control of sound transmission through a double glazed window by using arrangement of Helmholtz resonators (HRs)	9.6 dB reduction at 100 Hz (helicopter noise) 7 dB reduction at 63 Hz (highway noise)
Park [229]	2013	micro-perforated panel absorbers backed by Helmholtz resonators	reduction of 7.9 dB within 25–630 Hz
Zhao <i>et al</i> [84]	2016	mechanical impedance plate combined with Helmholtz resonators	with 3–5 resonators $\alpha > 0.9$ at around 390 Hz
Gai <i>et al</i> [230]	2016	microperforated panel mounted with helmholtz resonators	$\alpha > 0.7$ with 220–1000 Hz

where B_1 and B_2 refer to the modulus of the matrix and solid components, respectively. When the damping of the system is negligible, the effective bulk modulus of a Helmholtz resonator can be written as [236]:

$$\frac{1}{B_{\text{eff}}} = \frac{1}{B} \left(1 - \frac{\omega_{\text{sh}}^2}{\omega^2} \right)$$

where B is the bulk modulus of air, ω_{sh} is the cutoff frequency of the side hole, and ω is the angular of the harmonic excitation. As a result, acoustic metamaterials can achieve superior manipulation and control of the incident sound waves. In other words, they can conceal an object in terms of acoustics or redirect a soundwave to a desired direction opening simultaneously the way for further energy harvesting applications [89, 237, 238].

4.3.1. Metasurfaces—Membrane type metamaterials

Various studies have proposed acoustic metasurfaces capable to accomplish total absorption in a

narrow band of low frequencies range [89, 90] (table 21). However, the membrane-type acoustic metamaterials (MAMs) have raised moreover the scientific interest mainly due to their compact and lightweight nature [239]. The first MAM was introduced by Yang *et al* [240] and was characterized by negative dynamic mass, i.e. acceleration and spatially mean average force have opposite phase and hence materials comprising infinitesimal components can exhibit dynamics that deviate from Newton's second law [241], and almost perfect reflectance of acoustic waves within the 200–300 Hz frequency range. In the study of Lee *et al* [242], one-dimensional acoustic metamaterial with negative effective density using an array of very thin elastic membranes was found to highly block soundwaves from 0 to 735 Hz. Further on, Yang [243] developed a thin lightweight acoustic attenuation panel characterised by sound transmission loss greater than 40 dB in the broader range of 50–1000 Hz. Likewise, Mei *et al* [244] produced an elastic membrane decorated with

asymmetric rigid platelets able to ultimately absorb sound at specific frequencies in-between the range of 100–1000 Hz.

4.3.2. Metaporous structures

Furthermore, metamaterials have been developed for enhancing the sound absorption properties of porous structures, i.e. metaporous material (table 22). For instance, Yang [245] increased the sound absorption of a homogeneous porous layer by embedding rigid partitions and achieved a sound absorption coefficient higher than 0.7 above 2000 Hz. The same was reported by both studies of Zhou *et al* [246] and Yang *et al* [247], wherein the designed porous metasurface outperformed the conventional porous one in terms of acoustic absorption since the sound absorption coefficient reached values over 0.9 at frequencies higher than 1000 Hz.

5. Critical discussion

UHI and UNI, can be independently mitigated through a win-win approach: incorporation of smart skin with advanced physical properties into the built environment. However, coupling these properties in multifunctional surfaces than can act simultaneously towards the mitigation of both UHI and UNI is still a challenge and must be further investigated both in theory and practice. With regards to UHI, several passive material-based cooling techniques have been reported for being capable of substantially rejecting incident solar radiation. The main key performance indicators of the cool materials are typically the following:

- Magnitude of temperature abatement.
- Ageing.
- Winter penalty.
- Glare effect.
- Cost effectiveness.
- Environmental impact.

Nonetheless, the momentum of each cooling strategy is interconnected with the distinct physical and structural particularities of the implementation area; i.e. topography, meteorological profile, broader morphology, urban planning and anthropogenic heat [93]. In this regard, it is reported that white materials with high albedo values may substantially decrease their temperature during the summer period and can be cost-effective (table 23). However, they are subject to glaring issues due to their high reflectance in the visible region of the spectrum and moreover to inevitable ageing problems. As a result, in many cases, their implementation is prevented, especially to pedestrians and road pavements. The glaring penalty was partially solved with the introduction of the cool colored and fluorescent

materials due to their property of highly reflecting in the NIR spectrum. However, both undergo significant ageing issues. Similarly, thermochromic materials are vulnerable to ageing issues, however they have the main advantage of eliminating the winter penalty and decreasing the yearlong energy demand. Thus tackling the ageing issue of materials is, to date, of high importance. A potential solution however could be given through the further implementation of nano-scale thermochromic materials owing to their nature, though they still cannot be considered as a cost effective solution. On the contrary, an inexpensive solution excelling at the same time in terms of environmental impact are the natural or sustainable cool materials such as cool stones and grains.

In parallel, recent advances in noise mitigation techniques lead to proficient sound absorption on the audio frequency spectrum (table 24). Each sound absorption technique is characterized by different properties and thus it should be incorporated in the urban environment accordingly. For instance, porous materials are an ideal solution for exterior urban areas (i.e. pavements, building envelopes) owing to their fine sound absorption in a wide frequency range, their cost effectiveness and their low environmental impact since their components can be natural or organic. On the other hand, resonant absorbers excel in low frequencies which makes them ideal for indoors implementation. However, synergistic interactions in-between resonant and porous absorbers should be further investigated for urban applications. At the same time, metamaterials, can be regarded as the next generation of sound absorption materials since they are capable of not only totally absorbing sound but also redirecting the incident sound wave. That said, their mainly theoretical to date investigation and their high cost impede their urban application for the moment. However, further investigation should be carried out for cost effective metamaterial solutions in terms of sound absorption, since they could be pertinent for urban applications such as noise barriers.

Future focus should be given on merging rejection of solar radiation with sound absorption properties into one urban component (table 25). Under this scenario, urban materials comprising multiple layers should be developed. Mitigation mechanisms should be independently tuned within each layer which would synergistically act without compromising each other properties. Concerning UHI mitigation mechanism, special focus should be given to the external/upper layer of the surface. This layer directly interacts with incident radiation and hence its optical properties may regulate the overall thermal performance of the system. The UNI mitigation mechanism of the proposed material should be developed into the internal/bottom layer and hence will not affect solar rejection performance. The key attributes for not

Table 21. Metasurfaces—Membrane type metamaterials.

Study	Year	Purpose	Outcomes
Yang <i>et al</i> [240]	2008	membrane-type acoustic metamaterial	almost perfect reflectance of acoustic waves within 200–300 Hz
Lee <i>et al</i> [242]	2009	1-D metamaterial with negative effective density using an array of very thin elastic membranes	opaque within 0–735 Hz transparent above 735 Hz
Yang <i>et al</i> [243]	2010	thin membrane-type acoustic metamaterial	19.5 dB of internal sound transmission loss at around 200 Hz
Mei <i>et al</i> [244]	2012	thin elastic membranes decorated with designed patterns of rigid platelets	almost 99% absorption at 164 Hz and 645 Hz
Ma <i>et al</i> [89]	2014	metasurface that employs a novel hybrid resonance	Total absorption at 255, 309 and 420 Hz
Li and Assosuar [90]	2016	combination of a perforated plate and a coiled coplanar air chamber	total absorption around 125 Hz
Langfeldt <i>et al</i> [239]	2017	perforated membrane-type acoustic metamaterials	increased transmission loss over 25 dB within 100–1000 Hz

Table 22. Metaporous structures.

Study	Year	Purpose	Outcomes
Yang [245]	2015	metaporous layer was investigated in an effort to overcome the intrinsic thickness constraint of porous layers	$\alpha > 0.7$ above 2000 Hz
Yang <i>et al</i> [247]	2016	A set of rigid partitions of varying lengths inserted in a hard-backed porous layer	$\alpha > 0.9$ above 1000 Hz
Zhou <i>et al</i> [246]	2017	numerical study for a 2D acoustic metasurface fabricated using porous material	$\alpha > 0.8$ above 500 Hz

Table 23. UHI mitigation advances.

Type of material	Mitigation potential	Drawbacks		
		Ageing issues	Glaring issues	Winter penalty
classic cool	fine	✓	✓	✓
cool membranes	fine	✓	✓	✓
natural cool	good		✓	✓
cool colored	fine		✓	✓
retroreflective	fine	✓		✓
fluorescent	promising	✓		✓
thermochromic	fine	✓	✓	
nano-scale	superior			
recyclable	good	✓		✓

compromising the properties of the two layers are the aggregates and open pores size and flow resistivity of the external layer. All these properties should be chosen accordingly for ensuring enough air permeability and hence not compromise sound absorption of the internal/bottom layer. Depending on the nature of the application and the desired cooling and noise attenuation techniques, further layers may supplement the main two. For instance, if photoluminescent components are desired as the main cooling technique, they should be placed on the upper part of the external layer dedicated to UHI mitigation and could be backed by a sublayer of natural cool or cool membrane composites with high NIR reflectance.

Porous sound absorbers, e.g. natural fibers, inorganic foams, in unison with natural or sustainable cool materials should be considered as future solutions for tackling both UNI and UHI within pedestrian areas, cycle footpaths, parking lots, old town centers and so forth. In fact, an external layer comprising particles of an approximate size of 0.3–0.7 cm can function as good UHI mitigation mechanism that simultaneously allows the penetration of incident ambient sound-waves. Subsequently, a bottom layer developed with grains of an approximate size of 1.5–2.4 cm can ensure low flow resistivity (10,000–30,000 Ns/m⁴) and hence mitigate noise. Depending on the desired UNI mitigation magnitude, the porosity of the bottom layer should be well tuned above

Table 24. Noise mitigation advances.

Porous absorbers	Porous fibers	Natural fibers	fair absorption in mid-high frequencies cost effective good for extreme conditions, or for sound barriers in motorways nonwoven: low absorption to low-mid frequencies nanofibrous: good in low-mid frequencies
		Inorganic fibers	
		Synthetic fibers	
	Porous foams	Hybrid foams Organic foams	fair absorption in low-mid frequencies fair absorption in low-mid frequencies environmentally benign
Resonant absorbers	Inorganic foams		metal: good for extreme conditions cost effective when recyclable, combined with porous could excell in performance
	Membrane panel		tackle down the low frequency penalty of MPPs, effective only in its resonance peak
	Helmholtz resonators		superior sound absorption/control redirection of sound-wave
	Metamaterials		

Table 25. Next generation multifunctional surfaces.

UNI mitigation	UHI mitigation	Air pollution mitigation	Implementation field
porous natural fibers, inorganic foams	cool natural, recyclable	titanium/silicon dioxide zinc-oxide	pedestrians' pathwalks, parking areas, cycle paths
porous natural fibers, inorganic foams, membrane panels	cool natural, membranes	titanium/silicon dioxide zinc-oxide	roofs, facades
porous metal fibers, foams	cool colored, fluorescent	titanium/silicon dioxide zinc-oxide	roads
porous fibers, foams	nano- thermochromic	titanium/silicon dioxide zinc-oxide	building envelope

20%. Moreover, the thickness of the layer should be optimized according to the application. Concerning the absorption of sound-waves within low to mid frequencies, that mainly affect human health, an approximate thickness of 10 cm should be considered as reference [248]. Further increase of the thickness can lead to increased sound absorption, but within a narrower range at low frequencies.

The addition of cool-colored or photoluminescent particles into the external layer could minimize glare incidences, enhance the cooling potential, visibility and safety and/or satisfy aesthetic prerequisites. However, dispersing cool colorants either photoluminescent or not is not trivial [50]. Qualitative and quantitative dispersion assessments should be carried out through microscopy (electron and force), scattering (x-ray, neutron, and light), chemical spectroscopic methods, electrical and dielectric characterization, and mechanical spectroscopy, especially when nano-scale components are dispersed into polymer matrices [249]. In fact, parameters such as the dispersion technique, the size and, the center-to-center distance of the colorant particles may regulate the thermo-optical properties of the layer and hence material's temperature. However, reflective pavements should be developed with prudence and in accordance with the corresponding urban environment. Else, they may contribute towards increased mean radiant temperature and hence to pedestrian's

thermal discomfort [132]. On a similar approach, porous metal inorganic fibers/foams matched with modified asphalt including either cool pigments or photoluminescent components could be utilized in heavy traffic road pavements forming an inexpensive and environmentally benign solution. In that case, sound absorption should be specifically tuned within 500–1500 Hz which typically corresponds to the road-traffic noise. Moreover, a fine polishing of the surface may reduce the texture impact of tires.

Porous materials together with cool membranes or natural cool stones could be also placed on building facades and roofs. Under this scenario, sound absorption mechanism should be tuned into a wider frequency-range since community noise, e.g. noise originated from aircrafts, railways and motor vehicles, typically ranges between 50 Hz and 5000 Hz. The addition of an air gap behind the sound absorptive layer could increase sound absorption especially at mid and higher frequencies [250]. Also, sound absorption at low frequencies should be taken into consideration, especially with regards to office buildings. In fact, low-frequency noise originated from heating/cooling systems, ventilation systems, and fans or pumps in particular, together with indoor thermal discomfort have resulted in the Sick Building Syndrome (SBS) in many workplaces [251]. To that end, a layer comprising resonant sound absorbers embedded into porous matrices could moderate the

low frequency penalty of porous structures, and thus back a cool facade on office buildings.

Nano-scale thermochromics embedded in or placed above either porous foams or fibers can be further exploited for more advanced UHI and UNI mitigation solutions incorporated in facades or roofs of buildings. For example, adaptive structures that seasonally retune their UHI mitigation properties could be developed by dispersing cool, photoluminescent, photonic and so forth, nano-particles within a temperature responsive matrix, such as strain sensible polymers, biomimetic stretchable polymer opals or PCMs. Their cooling potential could be enhanced more if they are backed by a sublayer of selective absorption/emission spectra. In addition, the photocatalytic properties of zinc-oxide or titanium and silicon dioxide [252, 253] could be implemented in all proposed components for tackling air pollution in the lower heights of the urban environment, enhancing the cooling effect and adding self-cleaning properties. It should be noted that the present analysis focused on material-based solutions comprising mainly artificial components. Thus greenery and tree-based solutions were excluded from the analysis. However, since these type of solutions have been found capable of mitigating either UHI or UNI, they should be regarded and investigated as a supplementary component towards the moderation of urban discomfort [59].

Acknowledgment

Author's acknowledgments are due to the European Union's Horizon 2020 programme under grant agreement No 765057 (SAFERUP: Sustainable, Accessible, Safe, Resilient and Smart Urban Pavements. H2020 MSCA ITN-ETN project) and to the Italian project SOSCITTA supported by Fondazione Cassa di Risparmio di Perugia under grant agreement No 2 018.0499.026.

ORCID iD

A L Pisello  <https://orcid.org/0000-0002-4527-6444>

References

- [1] Mirzaei P A and Haghighat F 2010 Approaches to study urban heat island—abilities and limitations *Build. Environ.* **45** 2192–201
- [2] Ritchie H and Roser M 2018 Urbanization *Our World in Data* <https://ourworldindata.org/urbanization>
- [3] Nations United 2015 World urbanization prospects: The 2014 revision dept. of economic and social affairs—population division *Technical report* ST/ESA/SER. A/366 www.un.org/en/development/desa/policy/publications/2014-revision-world-urbanization-prospects.html#:~:{}:text=protect%20of%20the,population%20between%202014%20and%202050.
- [4] Oke T R 1982 The energetic basis of the urban heat island *Q. J. R. Meteorol. Soc.* **108** 1–24
- [5] Kaloustian N Aouad D, Battista G and Zinzi M 2018 Leftover spaces for the mitigation of urban overheating in municipal beirut *Climate* **6** 8
- [6] Chapman S, Watson J E M, Salazar A, Thatcher M and McAlpine C A 2017 The impact of urbanization and climate change on urban temperatures: a systematic review *Landsc. Ecol.* **32** 1921–35
- [7] Grimmond S U E 2007 Urbanization and global environmental change: local effects of urban warming *Geogr. J.* **173** 83–8
- [8] Vardoulakis S *et al* 2015 Impact of climate change on the domestic indoor environment and associated health risks in the uk *Environ. Int.* **85** 299–313
- [9] Santamouris M, Alevizos S M, Aslanoglou L, Mantzios D, Milonas P, Sarelli I, Karatasou S, Cartalis K and Paravantis J A 2014 Freezing the poor—indoor environmental quality in low and very low income households during the winter period in athens *Energy Build.* **70** 61–70
- [10] Bezaee A, Lomas K J and Firth S K 2013 National survey of summertime temperatures and overheating risk in english homes *Build. Environ.* **65** 1–17
- [11] Sakka A, Santamouris M, Livada I, Nicol F and Wilson M 2012 On the thermal performance of low income housing during heat waves *Energy Build.* **49** 69–77
- [12] Ramamurthy P, González J, Ortiz L, Arend M and Moshary F 2017 Impact of heatwave on a megacity: an observational analysis of new york city during july 2016 *Environ. Res. Lett.* **12** 054011
- [13] Gao Z, Hou Y and Chen W 2019 Enhanced sensitivity of the urban heat island effect to summer temperatures induced by urban expansion *Environ. Res. Lett.*
- [14] Tewari M, Yang J, Kusaka H, Palou F S, Watson C and Treinish L 2019 Interaction of urban heat islands and heat waves under current and future climate conditions and their mitigation using green and cool roofs in new york city and phoenix, arizona *Environ. Res. Lett.*
- [15] Dosio A, Mentaschi L, Fischer E M and Wyser K 2018 Extreme heat waves under 1.5 c and 2 c global warming *Environ. Res. Lett.* **13** 054006
- [16] Earl N, Simmonds I and Tapper N 2016 Weekly cycles in peak time temperatures and urban heat island intensity *Environ. Res. Lett.* **11** 074003
- [17] Yang J, Tham K W, Lee S E, Santamouris M, Sekhar C and Cheong D K W 2017 Anthropogenic heat reduction through retrofitting strategies of campus buildings *Energy Build.* **152** 813–22
- [18] Chrysoulakis N and Grimmond C S B 2016 Understanding and reducing the anthropogenic heat emission *Urban Climate Mitigation Techniques* (Abingdon: Routledge) pp 27–40 (http://centaur.reading.ac.uk/52736/1/Understanding_Reducing_Anthropogenic_Heat_Final_Draft.pdf)
- [19] Wong E, Hogan K, Rosenberg J and Denny A 2016 Reducing urban heat islands: Compendium of strategies urban heat island basics *Climate Protection Partnership Division in the US Environmental Protection Agency's Office of Atmospheric Programs* www.epa.gov/penalty-%20heatislands/heat-island-compendium
- [20] Doll D, Ching J K S and Kaneshiro J 1985 Parameterization of subsurface heating for soil and concrete using net radiation data *Bound.-Layer Meteorol.* **32** 351–72
- [21] Asaeda T, Ca V T and Wake A 1996 Heat storage of pavement and its effect on the lower atmosphere *Atmos. Environ.* **30** 413–27
- [22] Memon R A, Leung D Y and Chunho L 2008 A review on the generation, determination and mitigation of urban heat island *J. Environ. Sci.* **1** 020
- [23] Zhou B, Rybski D and Kropp Jurgen P 2017 The role of city size and urban form in the surface urban heat island *Sci. Rep.* **7** 4791

- [24] Manoli G, Fatichi S, Schl pfer M, Kailiang Y, Crowther T W, Meili N, Burlando P, Katul G G and Bou-Zeid E 2019 Magnitude of urban heat islands largely explained by climate and population *Nature* **573** 55–60
- [25] Gregory McPherson E 1998 Structure and sustainability of sacramento's urban forest *J. Arboriculture (USA)* **24** 174–90
- [26] Akbari H and Shea Rose L 2001 Characterizing the fabric of the urban environment: a case study of Salt Lake City, Utah *Technical Report* Lawrence Berkeley National Laboratory <https://escholarship.org/uc/item/0wk718sm>
- [27] Akbari H and Rose L S 2001 Characterizing the fabric of the urban environment: a case study of metropolitan Chicago, Illinois *Lawrence Berkeley National Laboratory Report LBNL-49275*, Berkeley, CA <https://escholarship.org/uc/item/7hq4p0z9>
- [28] Akbari H and Rose L S 2008 Urban surfaces and heat island mitigation potentials *J. Hum.-Environ. Syst.* **11** 85–101
- [29] Santamouris M 2013 Using cool pavements as a mitigation strategy to fight urban heat island—a review of the actual developments *Renew. Sust. Energ. Rev.* **26** 224–40
- [30] Pomerantz M and Akbari H 1998 Cooler paving materials for heat island mitigation *Proc. 1998 ACEEE summer study on energy efficiency in buildings* vol 9 p 135 www.osti.gov/biblio/8869
- [31] Kolokotsa D-D, Giannariakis G, Gobakis K, Giannarakis G, Synnefa A and Santamouris M 2018 Cool roofs and cool pavements application in acharnes, greece *Sustain. Cities Soc.* **37** 466–74
- [32] Stathopoulou M, Synnefa A, Cartalis C, Santamouris M, Karlessi T and Akbari H 2009 A surface heat island study of athens using high-resolution satellite imagery and measurements of the optical and thermal properties of commonly used building and paving materials *Int. J. Sustain. Energy* **28** 59–76
- [33] Synnefa A, Santamouris M and Livada I 2006 A study of the thermal performance of reflective coatings for the urban environment *Sol. Energy* **80** 968–81
- [34] Pisello A L and Cotana F 2014 The thermal effect of an innovative cool roof on residential buildings in italy: Results from two years of continuous monitoring *Energy Build.* **69** 154–64
- [35] Pisello A, Pignatta G, Castaldo V and Cotana F 2014 Experimental analysis of natural gravel covering as cool roofing and cool pavement *Sustainability* **6** 4706–22
- [36] Castaldo V L, Coccia V, Cotana F, Pignatta G, Pisello A L and Rossi F 2015 Thermal-energy analysis of natural “cool” stone aggregates as passive cooling and global warming mitigation technique *Urban Clim.* **14** 301–14
- [37] Doya M, Bozonnet E and Allard F 2012 Experimental measurement of cool facades’ performance in a dense urban environment *Energy Build.* **55** 42–50
- [38] Rosso F, Pisello A L, Castaldo V L, Fabiani C, Cotana F, Ferrero M and Jin W 2017 New cool concrete for building envelopes and urban paving: Optics-energy and thermal assessment in dynamic conditions *Energy Build.* **151** 381–92
- [39] Revel G M, Martarelli M, Emiliani M, Celotti L, Nadalini R, De Ferrari A, Hermanns S and Beckers E 2014 Cool products for building envelope—part ii: Experimental and numerical evaluation of thermal performances *Sol. Energy* **105** 780–91
- [40] Pisello A L, Fortunati E, Mattioli S, Cabeza L F, Barreneche C, Kenny J M and Cotana F 2016 Innovative cool roofing membrane with integrated phase change materials: Experimental characterization of morphological, thermal and optic-energy behavior *Energy Build.* **112** 40–8
- [41] Pisello A L, Fortunati E, Fabiani C, Mattioli S, Dominici F, Torre L, Cabeza L F and Cotana F 2017 Pcm for improving polyurethane-based cool roof membranes durability *Sol. Energy Mater. Sol. Cells* **160** 34–42
- [42] Chung M H and Park J C 2016 Development of pcm cool roof system to control urban heat island considering temperate climatic conditions *Energy Build.* **116** 341–8
- [43] Saffari M, Piselli C, de Gracia A, Pisello A L, Cotana F and Cabeza L F 2018 Thermal stress reduction in cool roof membranes using phase change materials (pcm) *Energy Build.* **158** 1097–105
- [44] Shilei L, Chen Y, Liu S and Kong X 2016 Experimental research on a novel energy efficiency roof coupled with pcm and cool materials *Energy Build.* **127** 159–69
- [45] Synnefa A, Karlessi T, Gaitani N, Santamouris M, Assimakopoulos D N and Papakatsikas C 2011 Experimental testing of cool colored thin layer asphalt and estimation of its potential to improve the urban microclimate *Build. Environ.* **46** 38–44
- [46] Santamouris M, Xirafi F, Gaitani N, Spanou A, Saliari M and Vassilakopoulou K 2012 Improving the microclimate in a dense urban area using experimental and theoretical techniques—the case of marousi, athens *Int. J. Vent.* **11** 1–16
- [47] Kyriakodis G E and Santamouris M 2018 Using reflective pavements to mitigate urban heat island in warm climates—results from a large scale urban mitigation project *Urban Clim.* **24** 326–39
- [48] Levinson R, Chen S, Ferrari C, Berdahl P and Slack J 2017 Methods and instrumentation to measure the effective solar reflectance of fluorescent cool surfaces *Energy Build.* **152** 752–65
- [49] Berdahl P, Chen S S, Destailats H, Kirchstetter T W, Levinson R M and Zalich M A 2016 Fluorescent cooling of objects exposed to sunlight—the ruby example *Sol. Energy Mater. Sol. Cells* **157** 312–17
- [50] Kousis I, Fabiani C, Gobbi L and Pisello A L 2020 Phosphorescent-based pavements for counteracting urban overheating – a proof of concept *Sol. Energy* **202** 540–52
- [51] Perez G, Allegro V R, Corroto M, Pons A and Guerrero A 2018 Smart reversible thermochromic mortar for improvement of energy efficiency in buildings *Constr. Build. Mater.* **186** 884–91
- [52] Jianying H and Yu X B 2019 Adaptive thermochromic roof system: Assessment of performance under different climates *Energy Build.* **192** 1–14
- [53] Fabiani C, Pisello A L, Bou-Zeid E, Yang J and Cotana F 2019 Adaptive measures for mitigating urban heat islands: The potential of thermochromic materials to control roofing energy balance *Appl. Energy* **247** 155–70
- [54] Rossi F, Castellani B, Presciutti A, Morini E, Filippini M, Nicolini A and Santamouris M 2015 Retroreflective fa ades for urban heat island mitigation: Experimental investigation and energy evaluations *Appl. Energy* **145** 8–20
- [55] Han Y, Taylor J E and Pisello A L 2015 Toward mitigating urban heat island effects: Investigating the thermal-energy impact of bio-inspired retro-reflective building envelopes in dense urban settings *Energy Build.* **102** 380–9
- [56] Yuan J, Farnham C and Emura K 2015 Development of a retro-reflective material as building coating and evaluation on albedo of urban canyons and building heat loads *Energy Build.* **103** 107–17
- [57] Zhang L, Deng Z, Liang L, Zhang Y, Meng Q, Wang J and Santamouris M 2019 Thermal behavior of a vertical green facade and its impact on the indoor and outdoor thermal environment *Energy Build.* **204** 109502
- [58] Wang J, Bao-Jie H, Wang H and Santamouris M 2019 Towards higher quality green building agenda—an overview of the application of green building techniques in china *Sol. Energy* **193** 473–93
- [59] Santamouris M *et al* 2018 Progress in urban greenery mitigation science—assessment methodologies advanced technologies and impact on cities *J. Civ. Eng. Manag.* **24** 638–71
- [60] Gao K and Santamouris M 2019 The use of water irrigation to mitigate ambient overheating in the built environment: Recent progress *Build. Environ.* **164** 106346
- [61] Pyrgou A, Santamouris M, Livada I and Cartalis C 2019 Retrospective analysis of summer temperature anomalies with the use of precipitation and evapotranspiration rates *Climate* **7** 104

- [62] Wang J, Meng Q, Zhang L, Zhang Y, Bao-Jie H, Zheng S and Santamouris M 2019 Impacts of the water absorption capability on the evaporative cooling effect of pervious paving materials *Build. Environ.* **151** 187–97
- [63] Gunawardena K R, Wells M J and Kershaw T 2017 Utilising green and bluespace to mitigate urban heat island intensity *Sci. Total Environ.* **584** 1040–55
- [64] Pijanowski B C, Villanueva-Rivera L J, Dumyahn S L, Farina A, Krause B L, Napoletano B M, Gage S H and Pieretti N 2011 Soundscape ecology: the science of sound in the landscape *Bioscience* **61** 203–16
- [65] European Environment Agency 2014 Noise in europe 2014
- [66] D'Alessandro F and Schiavoni S 2015 A review and comparative analysis of european priority indices for noise action plans *Sci. Total Environ.* **518** 290–301
- [67] Lambert J and Vallet M 1994 Study related to the preparation of a communication on a future ec noise policy: *final report* Institut National de Recherche sur les Transport et leur Sécurité (INRETS), Bron
- [68] Mathers C D and Loncar D 2006 Projections of global mortality and burden of disease from 2002 to 2030 *PLoS Med.* **3** e442
- [69] Decision No. 1386/2013/eu of the european parliament and of the council of 2 november 2013 on a general union environment action programme to 2020 'living well, within the limits of our planet 2013 *OJ L* **354**
- [70] World Health Organization 2018 *et al* Environmental noise guidelines for the european region
- [71] Auger N, Duplaix M, Bilodeau-Bertrand M, Ernest L and Smargiassi A 2018 Environmental noise pollution and risk of preeclampsia *Environ. Pollut.* **239** 599–606
- [72] Douglas O and Murphy E 2016 Source-based subjective responses to sleep disturbance from transportation noise *Environ. Int.* **92–93** 450–6
- [73] Hamoda M F 2008 Modeling of construction noise for environmental impact assessment *J. Constr. Dev. Cities.* **13** 79–89
- [74] Basner M, Babisch W, Davis A, Brink M, Clark C, Janssen S and Stansfeld S 2014 Auditory and non-auditory effects of noise on health *Lancet* **383** 1325–32
- [75] Halonen J I *et al* 2015 Road traffic noise is associated with increased cardiovascular morbidity and mortality and all-cause mortality in london *Eur. Heart J.* **36** 2653–61
- [76] The SMILE consortium 2003 Guidelines for road traffic noise abatement [https://ec.europa.eu/environment/life/project/Projects/index.cfm?fuseaction=protect\\$relax=\\$home.showFile&rep\protect\\$relax=\\$file&fil\protect\\$relax=\\$SMILE_guidelines_noise_en.pdf](https://ec.europa.eu/environment/life/project/Projects/index.cfm?fuseaction=protect$relax=$home.showFile&rep\protect$relax=$file&fil\protect$relax=$SMILE_guidelines_noise_en.pdf)
- [77] Berge T, Mioduszewski P, Ejsmont J *et al* 2017 Reduction of road traffic noise by source measures – present and future strategies *Noise Control Eng. J.* **65** 549–59
- [78] Bendtsen H, Fryd J, Sjøvold J, Bermlid J and Holck Skov R S 2018 Nordtyre—the potential for noise reduction using less noisy tyres and road surfaces www.euronoise2018.eu/docs/papers/455_EuroNoise2018.pdf
- [79] Murphy E and King E 2014 *Environmental Noise Pollution: Noise Mapping, Public Health and Policy* (New York: Elsevier) <https://doi.org/10.1016/C2012-0-13587-0>
- [80] Silva L T, Fonseca F, Rodrigues D and Campos A 2018 Assessing the influence of urban geometry on noise propagation by using the sky view factor *J. Environ. Plan. Manag.* **61** 535–52
- [81] Yuan M, Yin C, Sun Y and Chen W 2019 Examining the associations between urban built environment and noise pollution in high-density high-rise urban areas: A case study in wuhan, china *Sustain. Cities Soc.* **50** 101678
- [82] Zhai W, Xiang Y, Song X, Ang L Y L, Cui F, Lee H P and Li T 2018 Microstructure-based experimental and numerical investigations on the sound absorption property of open-cell metallic foams manufactured by a template replication technique *Mater. Des.* **137** 108–16
- [83] Cao L, Qiuxia F, Yang S, Ding B and Jianyong Y 2018 Porous materials for sound absorption *Compos. Commun.* **10** 25–35
- [84] Zhao X-D, Yong-Jie Y and Yuan-Jun W 2016 Improving low-frequency sound absorption of micro-perforated panel absorbers by using mechanical impedance plate combined with helmholtz resonators *Appl. Acoust.* **114** 92–8
- [85] Qiu X 2016 Principles of sound absorbers *Acoustic Textiles* (Berlin: Springer) pp 43–72
- [86] Tang X and Yan X 2017 Acoustic energy absorption properties of fibrous materials: a review *Composites A* **101** 360–80
- [87] Luo M 2017 Application of porous road materials in sponge city construction *Chem. Eng. Trans.* **62** 163–8
- [88] Rashidi S, Esfahani J A and Karimi N 2018 Porous materials in building energy technologies—a review of the applications, modelling and experiments *Renew. Sust. Energ. Rev.* **91** 229–47
- [89] Guancong M, Yang M, Xiao S, Yang Z and Sheng P 2014 Acoustic metasurface with hybrid resonances *Nat. Mater.* **13** 873
- [90] Yong Li and Assouar B M 2016 Acoustic metasurface-based perfect absorber with deep subwavelength thickness *Appl. Phys. Lett.* **108** 063502
- [91] Samarasinghe G, Lagisz M, Santamouris M, Yenneti K, Upadhyay A K, Suarez F D L P, Taunk B and Nakagawa S 2019 A visualized overview of systematic reviews and meta-analyses on low-carbon built environments: An evidence review map *Sol. Energy* **186** 291–9
- [92] Goodman L A 1961 Snowball sampling *Ann. Math. Stat.* **32** 148–70
- [93] Qin Y 2015 A review on the development of cool pavements to mitigate urban heat island effect *Renew. Sust. Energ. Rev.* **52** 445–59
- [94] Santamouris M 2014 Cooling the cities—a review of reflective and green roof mitigation technologies to fight heat island and improve comfort in urban environments *Sol. Energy* **103** 682–703
- [95] Zhang J, Zhang K, Liu J and Ban-Weiss G 2016 Revisiting the climate impacts of cool roofs around the globe using an earth system model *Environ. Res. Lett.* **11** 084014
- [96] Parker D E 2010 Urban heat island effects on estimates of observed climate change *Wiley Interdisciplinary Reviews: Climate Change* **1** 123–33
- [97] Santamouris M, Synnefa A, Kolokotsa D, Dimitriou V and Apostolakis K 2008 Passive cooling of the built environment—use of innovative reflective materials to fight heat islands and decrease cooling needs *Int. J. Low-Carbon Tec.* **3** 71–82
- [98] Hoffman M E and Givoni B 2007 *Effect of Building Materials on Internal Temperatures* (Haifa: Technion - Israel Institute of Technology)
- [99] Berg R and Quinn W 1978 Use of light colored surface to reduce seasonal thaw penetration beneath embankments on permafrost *Proc. of the second international symposium on cold regions engineering* University of Alaska 86–99
- [100] Taha H, Sailor D J and Akbari H 1992 High-albedo materials for reducing building cooling energy use *Technical Report* Lawrence Berkeley Laboratory
- [101] Akbari H, Gartland L and Konopacki S 1998 Measured energy savings of light colored roofs: Results from three California demonstration sites *Technical Report* Lawrence Berkeley National Laboratory, Environmental Energy Technologies Div.
- [102] Akridge J M 1998 High-albedo roof coatings—impact on energy consumption *ASHRAE Trans.* **104** 957
- [103] Doulos L, Santamouris M and Livada I 2004 Passive cooling of outdoor urban spaces. the role of materials *Sol. Energy* **77** 231–49
- [104] Santamouris M 2013 *Energy and Climate in the Urban Built Environment* (Abingdon: Routledge)
- [105] Ramamurthy P, Sun T, Rule K and Bou-Zeid E 2015 The joint influence of albedo and insulation on roof

- performance: An observational study *Energy Build.* **93** 249–58
- [106] Rosenfeld A H, Akbari H, Bretz S, Fishman B L, Kurn D M, Sailor D and Taha H 1995 Mitigation of urban heat islands: materials, utility programs, updates *Energy Build.* **22** 255–65
- [107] Rosenzweig C, Solecki W and Slosberg R 2006 Mitigating new york city's heat island with urban forestry, living roofs, and light surfaces *A report to the New York State Energy Research and Development Authority*
- [108] Lynn B H, Carlson T N, Rosenzweig C, Goldberg R, Druyan L, Cox J, Gaffin S, Parshall L and Civerolo K 2009 A modification to the noah lsm to simulate heat mitigation strategies in the new york city metropolitan area *J. Appl. Meteorol. Climatol.* **48** 199–216
- [109] Taha H 2008 Episodic performance and sensitivity of the urbanized mm5 (umms) to perturbations in surface properties in houston texas *Bound.-Layer Meteorol.* **127** 193–218
- [110] Zhou Y and Marshall Shepherd J 2010 Atlanta's urban heat island under extreme heat conditions and potential mitigation strategies *Nat. Hazards* **52** 639–68
- [111] Synnefa A, Dandou A, Santamouris M, Tombrou M and Soulakellis N 2008 On the use of cool materials as a heat island mitigation strategy *J. Appl. Meteorology and Climatology* **47** 2846–56
- [112] Ramamurthy P, Sun T, Rule K and Bou-Zeid E 2015 The joint influence of albedo and insulation on roof performance: A modeling study *Energy Build.* **102** 317–27
- [113] Morini E, Touchaei A, Castellani B, Rossi F and Cotana F 2016 The impact of albedo increase to mitigate the urban heat island in terni (italy) using the wrf model *Sustainability* **8** 999
- [114] Tsoka S, Theodosiou T, Tsikaloudaki K and Flourentzou F 2018 Modeling the performance of cool pavements and the effect of their aging on outdoor surface and air temperatures *Sustain. Cities Soc.* **42** 276–88
- [115] Tsoka S, Tsikaloudaki A and Theodosiou T 2018 Analyzing the envi-met microclimate model's performance and assessing cool materials and urban vegetation applications—a review *Sustain. Cities Soc.* **43** 55–76
- [116] Mitchell D *et al* 2016 Attributing human mortality during extreme heat waves to anthropogenic climate change *Environ. Res. Lett.* **11** 074006
- [117] Son J, Liu J C and Bell M L 2019 Temperature-related mortality: A systematic review and investigation of effect modifiers *Environ. Res. Lett.* **14** 073004
- [118] Macintyre H L and Heaviside C 2019 Potential benefits of cool roofs in reducing heat-related mortality during heatwaves in a european city *Environ. Int.* **127** 430–41
- [119] Pisello A L, Castaldo V L, Pignatta G, Cotana F and Santamouris M 2016 Experimental in-lab and in-field analysis of waterproof membranes for cool roof application and urban heat island mitigation *Energy Build.* **114** 180–90
- [120] Pisello A L, Castaldo V L, Piselli C, Fabiani C and Cotana F 2017 Thermal performance of coupled cool roof and cool façade: Experimental monitoring and analytical optimization procedure *Energy Build.* **157** 35–52
- [121] Gonçalves T D, Brito Vânia, Vidigal F, Matias L and Faria P 2015 Evaporation from porous building materials and its cooling potential *J. Mater. Civ. Eng.* **27** 04014222
- [122] Santamouris M, Synnefa A and Karlessi T 2011 Using advanced cool materials in the urban built environment to mitigate heat islands and improve thermal comfort conditions *Sol. Energy* **85** 3085–102
- [123] Levinson R, Berdahl P and Akbari H 2005 Solar spectral optical properties of pigments—part ii: survey of common colorants *Sol. Energy Mater. Sol. Cells* **89** 351–89
- [124] Levinson R, Akbari H and Reilly J C 2007 Cooler tile-roofed buildings with near-infrared-reflective non-white coatings *Build. Environ.* **42** 2591–605
- [125] Levinson R, Berdahl P, Akbari H, Miller W, Joedicke I, Reilly J, Suzuki Y and Vondran M 2007 Methods of creating solar-reflective nonwhite surfaces and their application to residential roofing materials *Sol. Energy Mater. Sol. Cells* **91** 304–14
- [126] Song J *et al* 2014 The effects of particle size distribution on the optical properties of titanium dioxide rutile pigments and their applications in cool non-white coatings *Sol. Energy Mater. Sol. Cells* **130** 42–50
- [127] Rosso F, Pisello A, Castaldo V, Ferrero M and Cotana F 2017 On innovative cool-colored materials for building envelopes: Balancing the architectural appearance and the thermal-energy performance in historical districts *Sustainability* **9** 2319
- [128] You Z, Zhang M, Wang J and Pei W 2019 A black near-infrared reflective coating based on nano-technology *Energy Build.* **205** 109523
- [129] Jin J, Liu L, Liu R, Wei H, Qian G, Zheng J, Xie W, Lin F and Xie J 2019 Preparation and thermal performance of binary fatty acid with diatomite as form-stable composite phase change material for cooling asphalt pavements *Constr. Build. Mater.* **226** 616–24
- [130] Xie N, Hui Li, Abdelhady A and Harvey J 2019 Laboratorial investigation on optical and thermal properties of cool pavement nano-coatings for urban heat island mitigation *Build. Environ.* **147** 231–40
- [131] Taleghani M, Sailor D and Ban-Weiss G A 2016 Micrometeorological simulations to predict the impacts of heat mitigation strategies on pedestrian thermal comfort in a los angeles neighborhood *Environ. Res. Lett.* **11** 024003
- [132] Middel A, Kelly Turner V, Schneider F A, Zhang Y and Stiller M 2020 Solar reflective pavements—a policy panacea to heat mitigation? *Environ. Res. Lett.* **15**
- [133] So B S, Jung Y H and Lee D W 2002 Shape design of efficient retroreflective articles *J. Mater. Process. Technol.* **130** 632–40
- [134] Pacheco-Torgal F, Granqvist C G, Jelle Børn P, Vanoli G P, Bianco N and Kurnitski J 2017 *Cost-Effective Energy Efficient Building Retrofitting: Materials, Technologies, Optimization and Case Studies* (Sawston: Woodhead Publishing)
- [135] Yuan J, Farnham C and Emura K 2015 A study on the accuracy of determining the retro-reflectance of retro-reflective material by heat balance *Sol. Energy* **122** 419–28
- [136] Akbari H and Touchaei A G 2014 Modeling and labeling heterogeneous directional reflective roofing materials *Sol. Energy Mater. Sol. Cells* **124** 192–210
- [137] Rossi F, Morini E, Castellani B, Nicolini A, Bonamente E, Anderini E and Cotana F 2015 Beneficial effects of retroreflective materials in urban canyons: Results from seasonal monitoring campaign *Journal of Physics: Conf. Series IOP Publishing* vol 655 p 012012 Bristol
- [138] Qin Y, Liang J, Tan K and Fanghua Li 2016 A side by side comparison of the cooling effect of building blocks with retro-reflective and diffuse-reflective walls *Sol. Energy* **133** 172–9
- [139] Yuan J, Emura K, Sakai H, Farnham C and Siqiang L 2016 Optical analysis of glass bead retro-reflective materials for urban heat island mitigation *Sol. Energy* **132** 203–13
- [140] Rossi F, Castellani B, Presciutti A, Morini E, Anderini E, Filippini M and Nicolini A 2016 Experimental evaluation of urban heat island mitigation potential of retro-reflective pavement in urban canyons *Energy Build.* **126** 340–52
- [141] Sakai H and Iyota H 2017 Development of two new types of retroreflective materials as countermeasures to urban heat islands *Int. J. Thermophys.* **38** 131
- [142] Manni M, Lobaccaro G, Goia F and Nicolini A 2018 An inverse approach to identify selective angular properties of retro-reflective materials for urban heat island mitigation *Sol. Energy* **176** 194–210
- [143] Pratico F G, Vaiana R and Noto S 2018 Photoluminescent road coatings for open-graded and dense-graded asphalts:

- Theoretical and experimental investigation *J. Mater. Civ. Eng.* **30** 04018173
- [144] Gutiérrez E I and Colorado H A 2020 Development and characterization of a luminescent coating for asphalt pavements *Characterization of Minerals, Metals and Materials* (Berlin: Springer) pp 511–19
- [145] Hosseini M and Akbari H 2014 Heating energy penalties of cool roofs: the effect of snow accumulation on roofs *Adv. Build. Energy Res.* **8** 1–13
- [146] Aitken D, Burkinshaw S M, Griffiths J and Towns A D 1996 Textile applications of thermochromic systems *Rev. Prog. Color. Relat. Top.* **26** 1–8
- [147] Yiping M, Zhu B and Keru W 2001 Preparation and solar reflectance spectra of chameleon-type building coatings *Sol. Energy* **70** 417–22
- [148] Garshasbi S and Santamouris M 2019 Using advanced thermochromic technologies in the built environment: Recent development and potential to decrease the energy consumption and fight urban overheating *Sol. Energy Mater. Sol. Cells* **191** 21–32
- [149] Yiping M, Zhang X, Zhu B and Keru W 2002 Research on reversible effects and mechanism between the energy-absorbing and energy-reflecting states of chameleon-type building coatings *Sol. Energy* **72** 511–20
- [150] Karlessi T, Santamouris M, Apostolakis K, Synnefa A and Livada I 2009 Development and testing of thermochromic coatings for buildings and urban structures *Sol. Energy* **83** 538–51
- [151] Karlessi T and Santamouris M 2013 Improving the performance of thermochromic coatings with the use of uv and optical filters tested under accelerated aging conditions *Int. J. Low-Carbon Technol.* **10** 45–61
- [152] Yu X B and Hu J. *et al* 2017 Polymeric thermochromic dye for improvement of asphalt pavement durability *Technical Report*, Ohio. Dept. of Transportation Office of Statewide Planning and Research <https://rosap.nhtl.bts.gov/view/dot/32189>
- [153] Garshasbi S, Santamouris M and Huang S 2018 Urban Nanophotonics and Micro/Nano Optics International Conference Rome
- [154] Mutanen J, Jaaskelainen T and Parkkinen J P S 2005 Thermochromism of fluorescent colors *Color Res. Appl.* **30** 163–71
- [155] Feng J, Gao K, Santamouris M, Shah K W and Ranzi G 2020 Dynamic impact of climate on the performance of daytime radiative cooling materials *Sol. Energy Mater. Sol. Cells* **208** 110426
- [156] Zeyghami M, Yogi Goswami D and Stefanakos E 2018 A review of clear sky radiative cooling developments and applications in renewable power systems and passive building cooling *Sol. Energy Mater. Sol. Cells* **178** 115–28
- [157] Santamouris M and Feng J 2018 Recent progress in daytime radiative cooling: Is it the air conditioner of the future? *Buildings* **8** 168
- [158] Zou C *et al* 2017 Metal-loaded dielectric resonator metasurfaces for radiative cooling *Adv. Opt. Mater.* **5** 1700460
- [159] Raman A P, Anoma M A, Zhu L, Rephaeli E and Fan S 2014 Passive radiative cooling below ambient air temperature under direct sunlight *Nature* **515** 540
- [160] Metz B, Davidson O R, Bosch P R, Dave R and Meyer L A 2007 Climate Change 2007: Mitigation of Climate Change www.ipcc.ch/report/ar4/wg3/
- [161] Zinzi M, Fasano G and Manilia E 2007 Properties and performance of an innovative reflective painting to reduce the cool-ing loads in buildings and mitigate the heat island effect in urban areas *Proc. of II Conf.–Building Low Energy Cooling and Advanced Ventilation Technologies in the 21st Century*, Crete, Greece vol 250
- [162] Ferrari C, Libbra A, Muscio A and Siligardi C 2013 Design of ceramic tiles with high solar reflectance through the development of a functional engobe *Ceram. Int.* **39** 9583–90
- [163] Kousis I, Fabiani C, Ercolanoni L and Pisello A L 2020 Using bio-oils for improving environmental performance of an advanced resinous binder for pavement applications with heat and noise island mitigation potential *Sustain. Energy Technol. Assess.* **39** 100706
- [164] Zinzi M and Fasano G 2009 Properties and performance of advanced reflective paints to reduce the cooling loads in buildings and mitigate the heat island effect in urban areas *Int. J. Sustain. Energy* **28** 123–39
- [165] Eijk J vd, Kosten C W and Kok W 1950 Sound absorption by porous materials I *Appl. Sci. Res.* **B** 1 50–62
- [166] Cox T and d'Antonio P 2016 *Acoustic Absorbers and Diffusers: Theory, Design and Application* (Boca Raton, FL: Crc Press)
- [167] Han F, Seiffert G, Zhao Y and Gibbs B 2003 Acoustic absorption behaviour of an open-celled aluminium foam *J. Phys. D: Appl. Phys.* **36** 294
- [168] Peng L 2017 13 - sound absorption and insulation functional composites *Advanced High Strength Natural Fibre Composites in Construction* (Woodhead Publishing) ed Fan M and Feng F pp 333–73
- [169] Allard J and Atalla N 2009 *Propagation of Sound in Porous Media: Modelling Sound Absorbing Materials 2e* (New York: Wiley)
- [170] Ersoy S and Haluk Kçük 2009 Investigation of industrial tea-leaf-fibre waste material for its sound absorption properties *Appl. Acoust.* **70** 215–20
- [171] Ismail L, Ghazali M I, Mahzan S and Zaidi A M A 2010 Sound absorption of arenga pinnata natural fiber *World Acad. Sci. Eng. Technol.* **67** 804–6
- [172] Fatima S and Mohanty A R 2011 Acoustical and fire-retardant properties of jute composite materials *Appl. Acoust.* **72** 108–14
- [173] Putra A, Abdullah Y, Efendy H, Mohamad W M F W and Salleh N L 2013 Biomass from paddy waste fibers as sustainable acoustic material *Adv. Acoust. Vib.* **2013** 605932
- [174] Berardi U and Iannace G 2015 Acoustic characterization of natural fibers for sound absorption applications *Build. Environ.* **94** 840–52
- [175] Asdrubali F, D'Alessandro F and Schiavoni S 2015 A review of unconventional sustainable building insulation materials *Sustain. Mater. Technol.* **4** 1–17
- [176] Peng L, Song B, Wang J and Wang D 2015 Mechanic and acoustic properties of the sound-absorbing material made from natural fiber and polyester *Adv. Mater. Sci. Eng.* **2015** 274913
- [177] Asdrubali F, Pisello A L, D'alessandro F, Bianchi F, Fabiani C, Cornicchia M and Rotili A 2016 Experimental and numerical characterization of innovative cardboard based panels: Thermal and acoustic performance analysis and life cycle assessment *Build. Environ.* **95** 145–59
- [178] Or K H, Putra A and Selamat M Z 2017 Oil palm empty fruit bunch fibres as sustainable acoustic absorber *Appl. Acoust.* **119** 9–16
- [179] Fabiani C, Coma Jà, Pisello A L, Perez G, Cotana F and Cabeza L F 2018 Thermo-acoustic performance of green roof substrates in dynamic hygrothermal conditions *Energy Build.* **178** 140–53
- [180] Putra A, Or K H and Selamat M Z 2018 Mohd Jailani Mohd Nor, Muhamad Haziq Hassan and Iwan Prasetyo. Sound absorption of extracted pineapple-leaf fibres *Appl. Acoust.* **136** 9–15
- [181] Santoni A, Bonfiglio P, Fausti P, Marescotti C, Mazzanti V, Mollica F and Pompili F 2019 Improving the sound absorption performance of sustainable thermal insulation materials: Natural hemp fibres *Appl. Acoust.* **150** 279–89
- [182] Zhang B and Tianning C 2009 Calculation of sound absorption characteristics of porous sintered fiber metal *Appl. Acoust.* **70** 337–46
- [183] Sun F, Chen H, Jiuhui W and Feng K 2010 Sound absorbing characteristics of fibrous metal materials at high temperatures *Appl. Acoust.* **71** 221–35

- [184] Meng H, Ao Q B, Ren S W, Xin F X, Tang H P and Lu T J 2015 Anisotropic acoustical properties of sintered fibrous metals *Compos. Sci. Technol.* **107** 10–17
- [185] Qingbo A, Jianzhong W, Huiping T, Hao Z, Jun M and Tengfei B 2015 Sound absorption characteristics and structure optimization of porous metal fibrous materials *Rare Metal Mat. Eng.* **44** 2646–50
- [186] Zhu J, Sun J, Tang H, Wang J, Qingbo A, Bao T and Song W 2016 Gradient-structural optimization of metal fiber porous materials for sound absorption *Powder Technol.* **301** 1235–41
- [187] Chen D, Hou L, Zhou W and Liu R 2017 Tri-dimensional reticulated porous material sintered by multi-tooth tool cutting-made copper fibers and investigation of its acoustical performances *Mater. Lett.* **194** 9–12
- [188] Lin J-H, Lin C-M, Huang C-C, Lin C-C, Hsieh C-T and Liao Y-C 2011 Evaluation of the manufacture of sound absorbent sandwich plank made of pet/tpu honeycomb grid/pu foam *J. Compos. Mater.* **45** 1355–62
- [189] Lou C-W, Lin J-H and Kuan-Hua S 2005 Recycling polyester and polypropylene nonwoven selvages to produce functional sound absorption composites *Text. Res. J.* **75** 390–4
- [190] Kosuge K, Takayasu A and Hori T 2005 Recyclable flame retardant nonwoven for sound absorption; ruba® *J. Mater. Sci.* **40** 5399–405
- [191] Suvari F, Ulcay Y, Maze B and Pourdeyhimi B 2013 Acoustical absorptive properties of spunbonded nonwovens made from islands-in-the-sea bicomponent filaments *J. Text. Inst.* **104** 438–45
- [192] Suvari F, Ulcay Y and Pourdeyhimi B 2016 Sound absorption analysis of thermally bonded high-loft nonwovens *Text. Res. J.* **86** 837–47
- [193] Zhu W, Nandikolla V and George B 2015 Effect of bulk density on the acoustic performance of thermally bonded nonwovens *J. Eng. Fiber. Fabr.* **10** 155892501501000316
- [194] Xiang H-fan, Tan S-xia, Xiao-lan Y, Long Y-hua, Zhang X-li, Zhao N and Jian X 2011 Sound absorption behavior of electrospun polyacrylonitrile nanofibrous membranes *Chin. J. Polymer Sci.* **29** 650
- [195] Kucukali-Ozturk M, Ozden-Yenigun E, Nergis B and Candan C 2017 Nanofiber-enhanced lightweight composite textiles for acoustic applications *J. Ind. Text.* **46** 1498–1510
- [196] Chang G *et al* 2016 Formation and self-assembly of 3d nanofibrous networks based on oppositely charged jets *Mater. Des.* **97** 126–30
- [197] Wu C M and Chou M H 2016 Polymorphism, piezoelectricity and sound absorption of electrospun pvdf membranes with and without carbon nanotubes *Compos. Sci. Technol.* **127** 127–33
- [198] Wu C M and Chou M H 2016 Sound absorption of electrospun polyvinylidene fluoride/graphene membranes *Eur. Polym. J.* **82** 35–45
- [199] Ying W *et al* 2017 Graphene foam/carbon nanotube/poly (dimethyl siloxane) composites as excellent sound absorber *Composites A* **102** 391–9
- [200] Bai P, Yang X, Shen X, Zhang X, Zhizhong Li, Yin Q, Jiang G and Yang F 2019 Sound absorption performance of the acoustic absorber fabricated by compression and microperforation of the porous metal *Mater. Des.* **167** 107637
- [201] Sung C H, Lee K S, Lee K S, Oh S M, Kim J H, Kim M S and Jeong H M 2007 Sound damping of a polyurethane foam nanocomposite *Macromol. Res.* **15** 443–8
- [202] Lee D K, Chen L, Sendjarevic A, Sendjarevic V, Frisch K C and Klempner D 1991 Effect of morphology on sound attenuation of flexible polymeric foams *J. Cell. Plast.* **27** 135–42
- [203] Chen S, Jiang Y, Chen J and Wang D 2015 The effects of various additive components on the sound absorption performances of polyurethane foams *A. Mater. Sci. Eng.* **2015** 317561
- [204] Sung G, Kim S K, Kim J W and Kim J H 2016 Effect of isocyanate molecular structures in fabricating flexible polyurethane foams on sound absorption behavior *Polym. Test.* **53** 156–64
- [205] Sung G, Kim J S and Kim J H 2018 Sound absorption behavior of flexible polyurethane foams including high molecular-weight copolymer polyol *Polym. Advan. Technol.* **29** 852–9
- [206] Choe H, Sung G and Kim J H 2018 Chemical treatment of wood fibers to enhance the sound absorption coefficient of flexible polyurethane composite foams *Compos. Sci. Technol.* **156** 19–27
- [207] Sung G and Kim J H 2017 Effect of high molecular weight isocyanate contents on manufacturing polyurethane foams for improved sound absorption coefficient *Korean J. Chem. Eng.* **34** 1222–8
- [208] Mosanenzadeh S G, Naguib H E, Park C B and Atalla N 2013 Development, characterization and modeling of environmentally friendly open-cell acoustic foams *Polym. Eng. Sci.* **53** 1979–89
- [209] Mosanenzadeh S G, Naguib H E, Park C B and Atalla N 2015 Design and development of novel bio-based functionally graded foams for enhanced acoustic capabilities *J. Mater. Sci.* **50** 1248–56
- [210] Huang K, Donghui Y, Siyuan H and Deping H 2011 Acoustic absorption properties of open-cell al alloy foams with graded pore size *J. Phys. D: Appl. Phys.* **44** 365405
- [211] Ligoda-Chmiel J, Śliwa R E and Potoczek M 2017 Flammability and acoustic absorption of alumina foam/tri-functional epoxy resin composites manufactured by the infiltration process *Composites B* **112** 196–202
- [212] Cuiyun D, Guang C, Xinbang X and Peisheng L 2012 Sound absorption characteristics of a high-temperature sintering porous ceramic material *Appl. Acoust.* **73** 865–71
- [213] Wang F, Hao G, Yin J, Xia Y, Zuo K, Liang H, Ning C, Yao D and Zeng Y 2017 Porous si3n4 fabrication via volume-controlled foaming and their sound absorption properties *J. Alloys Compd.* **727** 163–7
- [214] Arenas J P and Ugarte F 2016 A note on a circular panel sound absorber with an elastic boundary condition *Appl. Acoust.* **114** 10–17
- [215] Cobo P and de Espinosa F M 2013 Proposal of cheap microperforated panel absorbers manufactured by infiltration *Appl. Acoust.* **74** 1069–75
- [216] Maa D-Y 1998 Potential of microperforated panel absorber *J. Acoust. Soc. Am.* **104** 2861–6
- [217] Fuchs H V 2013 *Applied Acoustics: Concepts, Absorbers and Silencers for Acoustical Comfort and Noise Control: Alternative Solutions-Innovative Tools-Practical Examples* (Berlin: Springer)
- [218] Toyoda M and Takahashi D 2008 Sound transmission through a microperforated-panel structure with subdivided air cavities *J. Acoust. Soc. Am.* **124** 3594–603
- [219] Ning J F, Ren S W and Zhao G P 2016 Acoustic properties of micro-perforated panel absorber having arbitrary cross-sectional perforations *Appl. Acoust.* **111** 135–42
- [220] Dengke Li, Chang D and Liu B 2017 Enhanced low-to mid-frequency sound absorption using parallel-arranged perforated plates with extended tubes and porous material *Appl. Acoust.* **127** 316–23
- [221] Dengke Li, Chang D and Liu B 2016 Enhancing the low frequency sound absorption of a perforated panel by parallel-arranged extended tubes *Appl. Acoust.* **102** 126–32
- [222] Bucciarelli F, Malfense Fierro G P and Meo M 2019 A multilayer microperforated panel prototype for broadband sound absorption at low frequencies *Appl. Acoust.* **146** 134–44
- [223] Tang Y, Feihao Li, Xin F and Lu T J 2017 Heterogeneously perforated honeycomb-corrugation hybrid sandwich panel as sound absorber *Mater. Des.* **134** 502–12
- [224] Mao Q, Shengquan Li and Liu W 2018 Development of a sweeping helmholtz resonator for noise control *Appl. Acoust.* **141** 348–54

- [225] Chen K T, Chen Y H, Lin K Y and Weng C C 1998 The improvement on the transmission loss of a duct by adding helmholtz resonators *Appl. Acoust.* **54** 71–82
- [226] Tang S K 2005 On helmholtz resonators with tapered necks *J. Sound Vib.* **279** 1085–96
- [227] Estéve S J and Johnson M E 2002 Reduction of sound transmission into a circular cylindrical shell using distributed vibration absorbers and helmholtz resonators *J. Acoust. Soc. Am.* **112** 2840–8
- [228] Mao Q and Pietrzko S 2010 Experimental study for control of sound transmission through double glazed window using optimally tuned helmholtz resonators *Appl. Acoust.* **71** 32–8
- [229] Park S-H 2013 Acoustic properties of micro-perforated panel absorbers backed by helmholtz resonators for the improvement of low-frequency sound absorption *J. Sound Vib.* **332** 4895–4911
- [230] Gai X-L, Xing T, Xian-Hui Li, Zhang B and Wang W-J 2016 Sound absorption of microporated panel mounted with helmholtz resonators *Appl. Acoust.* **114** 260–5
- [231] Ren S W, Meng H, Xin F X and Lu T J 2016 Ultrathin multi-slit metamaterial as excellent sound absorber: Influence of micro-structure *J. Appl. Phys.* **119** 014901
- [232] Shen C, Jun X, Fang N X and Jing Y 2014 Anisotropic complementary acoustic metamaterial for canceling out aberrating layers *Phys. Rev. X* **4** 041033
- [233] Gracia-Salgado R, Torrent D and Sánchez-Dehesa J 2012 Double-negative acoustic metamaterials based on quasi-two-dimensional fluid-like shells *New J. Phys.* **14** 103052
- [234] Liu Z, Chan C T and Sheng P 2005 Analytic model of phononic crystals with local resonances *Phys. Rev. B* **71** 014103
- [235] Ying W, Lai Y and Zhang Z-Q 2007 Effective medium theory for elastic metamaterials in two dimensions *Phys. Rev. B* **76** 205313
- [236] Kushwaha M S, Halevi P, Martinez G, Dobrzynski L and Djafari-Rouhani B 1994 Theory of acoustic band structure of periodic elastic composites *Phys. Rev. B* **49** 2313
- [237] Oudich M, Senesi M, Badreddine Assouar M, Ruzenne M, Sun J-H, Vincent B, Hou Z and Tsung-Tsong W 2011 Experimental evidence of locally resonant sonic band gap in two-dimensional phononic stubbed plates *Phys. Rev. B* **84** 165136
- [238] Fleury R and Alù A 2013 Extraordinary sound transmission through density-near-zero ultranarrow channels *Phys. Rev. Lett.* **111** 055501
- [239] Langfeldt F, Kemsies H, Gleine W and Estorff O von 2017 Perforated membrane-type acoustic metamaterials *Phys. Lett.* **381** 1457–62
- [240] Yang Z, Mei J, Yang M, Chan N H and Sheng P 2008 Membrane-type acoustic metamaterial with negative dynamic mass *Phys. Rev. Lett.* **101** 204301
- [241] Milton G W and Willis J R 2007 On modifications of newton's second law and linear continuum elastodynamics *Proc. R. Soc. A* **463** 855–80
- [242] Lee S H, Park C M, Seo Y M, Wang Z G and Kim C K 2009 Acoustic metamaterial with negative density *Phys. Lett. A* **373** 4464–9
- [243] Yang Z, Dai H M, Chan N H, Ma G C and Sheng P 2010 Acoustic metamaterial panels for sound attenuation in the 50–1000 hz regime *Appl. Phys. Lett.* **96** 041906
- [244] Mei J, Guancong M, Yang M, Yang Z, Wen W and Sheng P 2012 Dark acoustic metamaterials as super absorbers for low-frequency sound *Nat. Commun.* **3** 756
- [245] Yang J, Lee J S and Kim Y Y 2015 Metaporous layer to overcome the thickness constraint for broadband sound absorption *J. Appl. Phys.* **117** 174903
- [246] Zhou J, Zhang X and Fang Y 2017 Three-dimensional acoustic characteristic study of porous metasurface *Compos. Struct.* **176** 1005–12
- [247] Yang J, Lee J S and Kim Y Y 2016 Multiple slow waves in metaporous layers for broadband sound absorption *J. Phys. D: Appl. Phys.* **50** 015301
- [248] Jafari M J, Monazam M R and Kazempour M 2018 Providing an optimal porous absorbent pattern to reduce mid to low-frequency sounds *J. Environ. Health Sci. Eng.* **16** 289–97
- [249] Krishnamoorti R 2007 Strategies for dispersing nanoparticles in polymers *MRS Bull.* **32** 341–7
- [250] Seddeq H S 2009 Factors influencing acoustic performance of sound absorptive materials *Aust. J. Basic Appl. Sci.* **3** 4610–17
- [251] Dhungana P and Chalise M 2020 Prevalence of sick building syndrome symptoms and its associated factors among bank employees in pokhara metropolitan, nepal *Indoor Air* **30** 244–50
- [252] Pinho L and Mosquera M J 2013 Photocatalytic activity of tio2–sio2 nanocomposites applied to buildings: Influence of particle size and loading *Appl. Catal. B* **134–135** 205–21
- [253] Rocha Segundo I G D, Lages Dias E A, Pereira Fernandes F D, de Freitas E F, Costa M F and Carneiro J O 2019 Photocatalytic asphalt pavement: the physicochemical and rheological impact of tio2 nano/microparticles and zno microparticles onto the bitumen *Road Mater. Pavement Des.* **20** 1452–67